













The Mediator complex subunit MED25 interacts with HDA9 and PIF4 to regulate thermomorphogenesis

Umidjon Shapulatov ^{1,2}, Martijn van Zanten ³, Mark van Hoogdalem ^{1,†}, Mara Meisenburg ¹, Alexander van Hall,¹ Iris Kappers ¹, Carlo Fasano ⁴, Paolo Facella ⁴, Chi Cheng Loh ², Giorgio Perrella ^{4,‡} and Alexander van der Krol ^{1,*}

- 1 Laboratory of Plant Physiology, Wageningen University & Research, Droevendaalsesteeg 1, 6708 PB Wageningen, The Netherlands
- 2 Temasek Life Science Laboratory, 1 Research Link, National University of Singapore, Singapore 117604, Singapore
- 3 Plant Stress Resilience, Institute of Environmental Biology, Utrecht University, Padualaan 8, 3584 CH Utrecht, the Netherlands
- 4 Italian National Agency for New Technologies, Energy and Sustainable Economic Development (ENEA), Trisaia Research Centre, S.S. Ionica, km 419.5, 75026 Rotondella (Matera), Italy

*Author for correspondence: Sander.vanderKrol@wur.nl

[†]Present address: Business Unit Greenhouse Horticulture, Wageningen University & Research, Droevendaalsesteeg 1, 6708PB Wageningen, The Netherlands

[‡]Present address: Department of Biosciences, University of Milan, 20133 Milano, Italy

A.v.d.K., M.v.Z., and G.P. designed the research; U.S., M.v.H., M.M., C.F., and P.F. C.C.L. performed the research; G.P., U.S., A.v.d.K., M.v.Z., M.M., and I.K. analyzed the data; and U.S. and A.v.d.k. wrote the paper.

The author responsible for distribution of materials integral to the findings presented in this article in accordance with the policy described in the Instructions for Authors (<https://academic.oup.com/plphys/pages/General-Instructions>) is Alexander van der Krol.

Abstract

Thermomorphogenesis is, among other traits, characterized by enhanced hypocotyl elongation due to the induction of auxin biosynthesis genes like *YUCCA8* by transcription factors, most notably PHYTOCHROME INTERACTING FACTOR 4 (PIF4). Efficient binding of PIF4 to the *YUCCA8* locus under warmth depends on HISTONE DEACETYLASE 9 (HDA9) activity, which mediates histone H2A.Z depletion at the *YUCCA8* locus. However, HDA9 lacks intrinsic DNA-binding capacity, and how HDA9 is recruited to *YUCCA8*, and possibly other PIF4-target sites, is currently not well understood. The Mediator complex functions as a bridge between transcription factors bound to specific promoter sequences and the basal transcription machinery containing RNA polymerase II. Mutants of Mediator component Mediator25 (MED25) exhibit reduced hypocotyl elongation and reduced expression of *YUCCA8* at 27°C. In line with a proposed role for MED25 in thermomorphogenesis in *Arabidopsis thaliana*, we demonstrated an enhanced association of MED25 to the *YUCCA8* locus under warmth and interaction of MED25 with both PIF4 and HDA9. Genetic analysis confirmed that MED25 and HDA9 operate in the same pathway. Intriguingly, we also showed that MED25 destabilizes HDA9 protein. Based on our findings, we propose that MED25 recruits HDA9 to the *YUCCA8* locus by binding to both PIF4 and HDA9.

Introduction

Thermomorphogenesis is an inclusive term that describes diverse growth responses, such as hypocotyl- and petiole

elongation, that plants exhibit when exposed to mildly elevated temperatures. Altogether this results in an altered architecture that helps mitigate the negative effects of warmth (Crawford et al., 2012; Quint et al., 2016; Casal and

Received March 1, 2022. Accepted November 1, 2022. Advance access publication December 20, 2022

© The Author(s) 2022. Published by Oxford University Press on behalf of American Society of Plant Biologists.

This is an Open Access article distributed under the terms of the Creative Commons Attribution-NonCommercial-NoDerivs licence (<https://creativecommons.org/licenses/by-nc-nd/4.0/>), which permits non-commercial reproduction and distribution of the work, in any medium, provided the original work is not altered or transformed in any way, and that the work is properly cited. For commercial re-use, please contact journals.permissions@oup.com

Open Access

Balasubramanian, 2019). Thermomorphogenesis is among other factors mediated by the transcription factor PHYTOCHROME INTERACTING FACTOR 4 (PIF4), which may be considered a central signaling hub in the warm temperature response network (Koini et al., 2009; Sun et al., 2012). Recently, PHYTOCHROME INTERACTING FACTOR 7 (PIF7) has been described as more dominant, especially where it involves crosstalk with light signaling (Burko et al., 2022). High temperatures lead to the induction of *PIF4* transcription and light-activated Phytochrome B (PhyB) is able to interact directly with PIF4, thereby phosphorylating the transcription factor, which results in its degradation through the 26S proteasome pathway (Huq and Quail, 2002; Lorrain et al., 2008). PIF4 not only mediates high-temperature-induced elongation growth, but also temperature-mediated activation of flowering, through direct regulation of the expression of FLOWERING LOCUS T (FT) (Kumar et al., 2012). PIF4 also coordinates the balance between temperature-mediated growth and immunity (Gangappa et al., 2017).

Up to now, two main mechanisms have been described for the upregulation of *PIF4* transcription under warmth: expression of *PIF4* is temporarily repressed by the circadian clock-related Evening Complex (EC), and this repression is released under warmth (Nusinow et al., 2011). Subsequently, the expression of *PIF4* is further stimulated by brassinosteroid (BR)-activated transcription factor BRASSINAZOLE-RESISTANT 1 (BZR1) (Ibanez et al., 2018) in a positive feedback loop, where PIF4 activates BR biosynthesis genes under warmth (Ibanez et al., 2018). In addition, the activity of the PIF4 protein at its direct target genes like the auxin biosynthesis gene *YUCCA8* is regulated by the clock through the EC component EARLY FLOWERING 3 (ELF3) (Box et al., 2015; Raschke et al., 2015). This induction of auxin biosynthesis and downstream signaling is required for the elongation growth responses that are triggered by high temperatures (Koini et al., 2009; Franklin et al., 2011; Sun et al., 2012; Bours et al., 2013; Bours et al., 2015; Kim et al., 2020), as well as during the shade avoidance response induced by elevated far-red (FR) light conditions (Muller-Moule et al., 2016; Ma and Li, 2019).

In concert with PIF4, the action of the histone-modifying enzyme HISTONE DEACETYLASE 9 (HDA9) contributes to thermomorphogenesis (van der Woude et al., 2019). Although histone deacetylation is usually linked to gene repression (Tian et al., 2005; Perrella et al., 2013), in the context of thermomorphogenesis, HDA9 activity allows for transcriptional activation of *YUCCA8*, as HDA9 action is required for eviction of the repressive histone variant H2A.Z from the *YUCCA8* locus, which is followed by PIF4 binding (van der Woude et al., 2019). HDA9 is part of a larger multiprotein complex and interacts with among other proteins POWERDRESS (PWR) (de Rooij et al., 2020; Perrella et al., 2022). PWR is involved in deacetylation events of histones at the +1 nucleosomes of both *PIF4* and *YUCCA8* and this deacetylation is required for the upregulation of these genes during thermomorphogenesis (Tasset et al., 2018). In

establishing seedlings, HDA9-LUC fusion protein activity is sharply increased at the onset of light at high temperatures (van der Woude et al., 2019), and HDA9 nuclear accumulation and chromatin association are dependent on PWR (Chen et al., 2016). However, since HDA9 nor PWR can bind directly to DNA, it is not clear how PWR and HDA9 are recruited to the *PIF4* (PWR) and *YUCCA8* (both PWR and HDA9) loci during thermomorphogenesis.

Mediator of RNA polymerase II transcription (Mediator) is a multi-subunit protein complex originally discovered in yeast (*Saccharomyces cerevisiae*) that functions as a co-regulator of transcription (Flanagan et al., 1991; Kim et al., 1994). The Mediator complex is highly conserved and comprises 25 subunits in budding yeast, 30 subunits in metazoans, and 34 subunits in plants (Soutourina, 2018). The Mediator complex functions as a bridge between gene-specific regulatory proteins and the transcription initiation complex (TIC) containing RNA Pol II (Kidd et al., 2011; Samanta and Thakur, 2015). Of the different protein subunits forming the Mediator complex, MEDIATOR25/PHYTOCHROME AND FLOWERING TIME 1 (MED25/PFT1) is specific for metazoans and plants and is absent in yeast and algae (Elfving et al., 2011; Kidd et al., 2011). Plant MED25 was initially identified as a gene affecting phytochrome signaling and flowering time and was therefore named PHYTOCHROME AND FLOWERING TIME 1 (PFT1) (Cerdan and Chory, 2003). Currently, MED25 has been linked to, for instance, transcriptional regulation related to methyl-jasmonate (MeJA) signaling (Kidd et al., 2010; Cevik et al., 2012), flowering (Inigo, Alvarez, et al., 2012), stress responses (Elfving et al., 2011), and floral organ size (Xu and Li, 2011). MED25/PFT1 is also required for the sugar-hypersensitive hypocotyl elongation phenotype of a UDP-arabinose synthesis mutant of HIGH SUGAR RESPONSE8 (*hsr8-1*) (Seguela-Arnaud et al., 2015) and is important for defense against virus infection, as the RNAi pathway is weakened in *med25* mutants (Hussein et al., 2020).

In *Arabidopsis* (*Arabidopsis thaliana*), MED25/PFT1 interacts with a specific subset of transcription factors, as determined by yeast-two-hybrid (Y2H) assays, bimolecular fluorescence complementation (BiFC) analysis and split-luciferase (split-LUC) assays (see Table 1 and references therein). *Arabidopsis* transcription factors PIF4 and BZR1 were previously tested for interaction with MED25 protein in yeast-two-hybrid assays. However, in these assays, they were not identified as MED25 targets (Ou et al., 2011).

The MED25/PFT1 mutant (*pft1-2*) does not show reduced hypocotyl elongation under low-red and far-red light, but *pft1-2* exhibited an increase in light sensitivity under strong continuous red light (Kidd et al., 2009; Klose et al., 2012). Young *pft1-2* mutant rosette plants grown under white light are smaller than their corresponding wild type (Cerdan and Chory, 2003). By contrast, the *pft1-2* mutant has markedly larger floral organ size, which is attributed to prolonged cell proliferation and elongation of petals (Xu and Li, 2011). A role of MED25/PFT1 in hypocotyl elongation in response to light intensity cues was confirmed by the dominant mutation

Table 1 Transcription factors (TFs) that can interact with Arabidopsis MED25

#	TF	ID acc.	TF family	Responses	Methods	Ref
1	DREB2A	AT5G05410	AP2; ERF	drought	Y2H	(Elfving et al., 2011; Cevik et al., 2012)
2	RAP2.2	AT3G14230	AP2; ERF	ethylene	Y2H	(Ou et al., 2011)
3	ERF95	AT3G23220	AP2; ERF	ethylene	Y2H	(Ou et al., 2011)
4	TDR1	AT3G23230	AP2; ERF	ethylene	Y2H	(Ou et al., 2011; Cevik et al., 2012)
5	ERF1	AT3G23240	AP2; ERF	ethylene	Y2H	(Ou et al., 2011; Cevik et al., 2012)
6	-	AT4G18450	AP2; ERF	ethylene	Y2H	(Ou et al., 2011)
7	ERF109	AT4G34410	AP2; ERF	ethylene	Y2H	(Ou et al., 2011)
8	ORA59	AT1G06160	AP2; ERF	ethylene	Y2H	(Cevik et al., 2012)
9	ERF15	AT2G31230	AP2; ERF	ethylene	Y2H	(Cevik et al., 2012)
10	WIN1	AT1G15360	AP2; ERF	ethylene	-	(Zhu et al., 2014)
11	EIN3	AT3G20770	EIN3; EIL	ethylene	Y2H, BiFC, Split-LUC	(Yang et al., 2014)
12	EIL1	AT2G27050	EIN3; EIL	ethylene	Y2H, BiFC, Split-LUC	(Yang et al., 2014)
13	BZS1	AT4G39070	DBB	BR signaling	Y2H	(Ou et al., 2011; Cevik et al., 2012)
14	WRKY10	AT1G55600	WRKY	-	Y2H	(Cevik et al., 2012)
15	MYB104	AT2G26950	MYB	-	Y2H	(Cevik et al., 2012)
16	ZFHD1	AT1G69600	ZF-HD	Salt, drought, ABA	Y2H	(Elfving et al., 2011)
17	POSF21	AT2G31370	bZIP	Salt stress	Y2H	(Cevik et al., 2012)
18	PHL1	AT5G29000	Myb/SANT	P starvation	Y2H	(Elfving et al., 2011; Ou et al., 2011)
19	MYC2	AT1G32640	bHLH	JA signaling	Y2H	(Cevik et al., 2012)
20	MYC3	AT5G46760	bHLH	JA signaling	IP	(Zhang et al., 2015)
21	MYC4	AT4G17880	bHLH	JA signaling	Y2H	(Cevik et al., 2012)
22	ABI5	AT2G36270	bZIP	ABA signaling	BiFC	(Chen et al., 2012)
23	ARF7	AT5G20730	B3; ARF	Auxin signaling	Y2H	(Ito et al., 2016)
24	ARF19	AT1G19220	B3; ARF	Auxin signaling	Y2H	(Ito et al., 2016)
25	TCP4	AT3G15030	TCP	Flowering time	Split-LUC	(Liu et al., 2017)
26	FBH1	AT1G35460	bHLH	Flowering time	Split-LUC	(Liu et al., 2017)
27	PIF4	AT2G43010	bHLH	Growth	Split-LUC, BiFC	this study
29	BZR1	AT1G75080	BES1	BR signaling	Split-LUC	this study

TF = transcription factor; ID acc = Arabidopsis gene identifier; Y2H = yeast two-hybrid assay; Split-LUC = biomolecular luciferase luminescence complementation; BiFC = biomolecular fluorescence complementation; Ref = reference.

PFT1^{eid3} (Klose et al., 2012). It was shown that PFT1^{eid3} enhances light sensitivity downstream of phytochrome A (phyA) and modulates phyB function, resulting in the expression of light-regulated genes in darkness (Klose et al., 2012). In tomato (*Solanum lycopersicum*), MED25 is involved in FR light (shade)-induced hypocotyl elongation (Hartman, 2020). In contrast to Arabidopsis (Ou et al., 2011), MED25 was shown to physically interact with PIF4 in tomato, and CHIP experiments demonstrated that MED25 shows increased association with the tomato YUCCA8 locus under increased shade conditions (Sun et al., 2020). By contrast, the silencing of MED25 in rice (*Oryza sativa*) appears not to have an apparent effect on plant growth and development (Zhang et al., 2021).

As indicated earlier, auxin has an important function in elongation responses (Gray et al., 1998; Delker et al., 2014; Bours et al., 2015; Ibanez et al., 2018). MED25 was proposed to play a role downstream of auxin signaling, as MED25 interacts with auxin response factors (ARFs) (Ito et al., 2016). However, the role of MED25 protein is pleiotropic and MED25 interacts with a broader range of transcription factors involved in auxin, jasmonic acid, ABA, and ethylene hormone-signaling pathways (Kazan, 2017). Therefore, in the *pft1-2* mutant, multiple hormone-signaling pathways are affected, all of which potentially could affect hypocotyl elongation responses under specific environmental conditions (Castroverde and Dina, 2021).

Here, we investigated the role of Arabidopsis MED25 in high-temperature signaling and thermomorphogenesis. We demonstrate that, like tomato MED25, Arabidopsis MED25 can interact with PIF4. At the chromatin level, we found increased binding of MED25 to the *PIF4* and *YUCCA8* loci under elevated temperature conditions. Moreover, we found that MED25 also interacts with HDA9. Interestingly, both PIF4 and HDA9 interact with the same C-terminal *polyQ*-domain of MED25. However, the binding of PIF4 and HDA9 to MED25 may not be mutually exclusive. Taken together, we present a mechanism by which MED25 recruits HDA9 to PIF4 target sites during mildly elevated temperatures.

Results

MED25 affects Arabidopsis growth

To investigate the role of MED25 in the growth responses of *Arabidopsis thaliana*, the leaf area and leaf petiole length of wild-type (WT) and MED25 mutant (*pft1-2*) rosette plants, grown at control temperature (22°C), were quantified. Results show that the effects of MED25 are complex, as young leaves are smaller, while older leaves are larger in *pft1-2* compared to WT (Supplemental Figure 1A). This could be the result of initially reduced expansion combined with a prolonged period of leaf expansion in *pft1-2* compared to WT. However, the average rosette area of 3–9-week-old

pft1-2 mutants is smaller than that of WT plants, which can be mainly attributed to the reduced leaf petiole length of the largest leaves in the *pft1-2* mutant (Supplemental Figure 1, B and C). To test whether MED25 also affects thermomorphogenesis, hypocotyl length was quantified of WT, two mutant alleles of MED25 (*pft1-2* and *pft1-3*), and plants overexpressing MED25 (35S:MED25myc, hereafter called MED25 OE) grown at control temperature (22°C) and warm temperature conditions (27°C) in short-day photoperiod (8 h light/16 h darkness). The hypocotyl length of WT and *pft1* mutants is similar at 4 days post-germination (Supplemental Figure 1D) but differs 8 days post-germination. At 22°C, hypocotyl length of *pft1-2* was similar to WT, whereas *pft1-3* was slightly longer, and the MED25 OE line slightly shorter, than WT (Figure 1A, Supplemental Figure 1E). However, when grown at 27°C the average hypocotyl lengths of both *pft1-2* and *pft1-3* and of MED25 OE were significantly shorter than those of WT (Figure 1A, Supplemental Figure 1E). The ratio of hypocotyl length at 27°C over 22°C shows that both *med25* mutants exhibit a consistently reduced sensitivity to heat (Figure 1B and Supplemental Figure 1E). The effect of mutation of MED25 and overexpression of MED25 both result in reduced elongation at 27°C

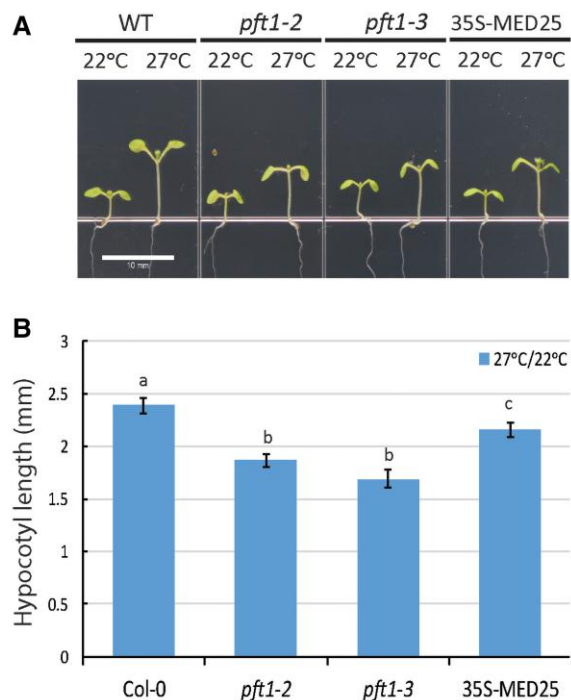


Figure 1 MED25 affects growth of Arabidopsis during thermomorphogenesis. A, image of representative WT, *pft1-2*, *pft1-3*, and MED25 OE 8-day old seedling grown at 22°C or 27°C. B, Ratio of hypocotyl length of seedlings grown at 22°C or 27°C. Bars are means \pm SE ($n = 25$ seedlings). Different letters indicate significant differences according to the Tukey HSD post hoc test ($P < 0.001$). Additional experiment is reported in the supplemental material, displaying similar results (Supplemental Figure 1E).

compared to WT. Overall, these results suggest a complex role for MED25 during growth at elevated temperatures.

MED25 limits expression of PIF4

Elongation responses during thermomorphogenesis are governed by the activity of the transcription factor PIF4. To test the effect of MED25 on the (diurnal) expression of PIF4, a *pPIF4:Luciferase* (LUC) reporter line was constructed in the Col-0 (WT) background and subsequently crossed into the *pft1-2* mutant background, thus allowing for direct comparison of the LUC activity of the same transgene in the different genetic backgrounds. *In planta* LUC activity was imaged and quantified (van Hoogdalem et al., 2021). Results show that *pPIF4:LUC* activity is higher in the *pft1-2* mutant background compared to WT (Figure 2, A and B). Moreover, the relative increase in *pPIF4:LUC* expression during a 12 h light/12 h darkness cycle is larger toward dusk, indicating that the suppressive effect of MED25 likely occurs primarily at the second half of the day (Figure 2C). To confirm these results, endogenous PIF4 mRNA levels were quantified in 3-week-old WT and *pft1-2* plants by RT-qPCR. Samples were harvested at zeitgeber time (ZT) = 8 h near the peak of PIF4 expression (Figure 2C). Again, at 22°C the expression of PIF4 is higher in the *pft1-2* mutant background compared to that in WT (Figure 2D). Moreover at 27°C, the expression of PIF4 in WT increases as expected (Koini et al., 2009; Ibanez et al., 2018), but PIF4 expression increased even more in the *pft1-2* mutant background as compared to WT (Figure 2D).

The effect of MED25 on PIF4 expression was further confirmed *in planta* in a transient expression assay in *N. benthamiana* leaves, using a *pPIF4:LUC* reporter and a 35S:MED25 effector construct. Results of LUC activity assessment show that also in this assay MED25 suppresses expression from the PIF4 promoter (Figure 2E). Next, the activity of transiently expressed *pPIF4:LUC* with MED25 OE or with empty vector (EV) was monitored during a 12 h light/12 h darkness cycle and also in this transient assay in *N. benthamiana* leaves, the relative suppression of *pPIF4:LUC* activity by MED25 increases toward the end of day (Figure 2F).

Combined, these results indicate that MED25 limits PIF4 expression at both temperatures. We note that the expression of PIF4 in *pft1-2* at 22°C is similar to the expression of PIF4 in WT at 27°C, while also at 27°C expression of PIF4 is significantly higher in *pft1-2* compared to WT (Figure 2D). However, this increased expression of PIF4 in *pft1-2* corresponds with only a minor—but significant—increase in hypocotyl elongation at 22°C (Figure 1B). Moreover, while PIF4 expression in *pft1-2* at 27°C is higher than in WT at 27°C, the hypocotyl elongation in *pft1-2* at 27°C is much reduced compared to WT under the same conditions (Supplemental Figure 1D). Thus, although increased PIF4 expression associates with longer hypocotyls in wild type (Koini et al., 2009; Ibanez et al., 2018), in *pft1-2* we see almost no effect of PIF4 expression (at 22°C) on hypocotyl length or the effect is even

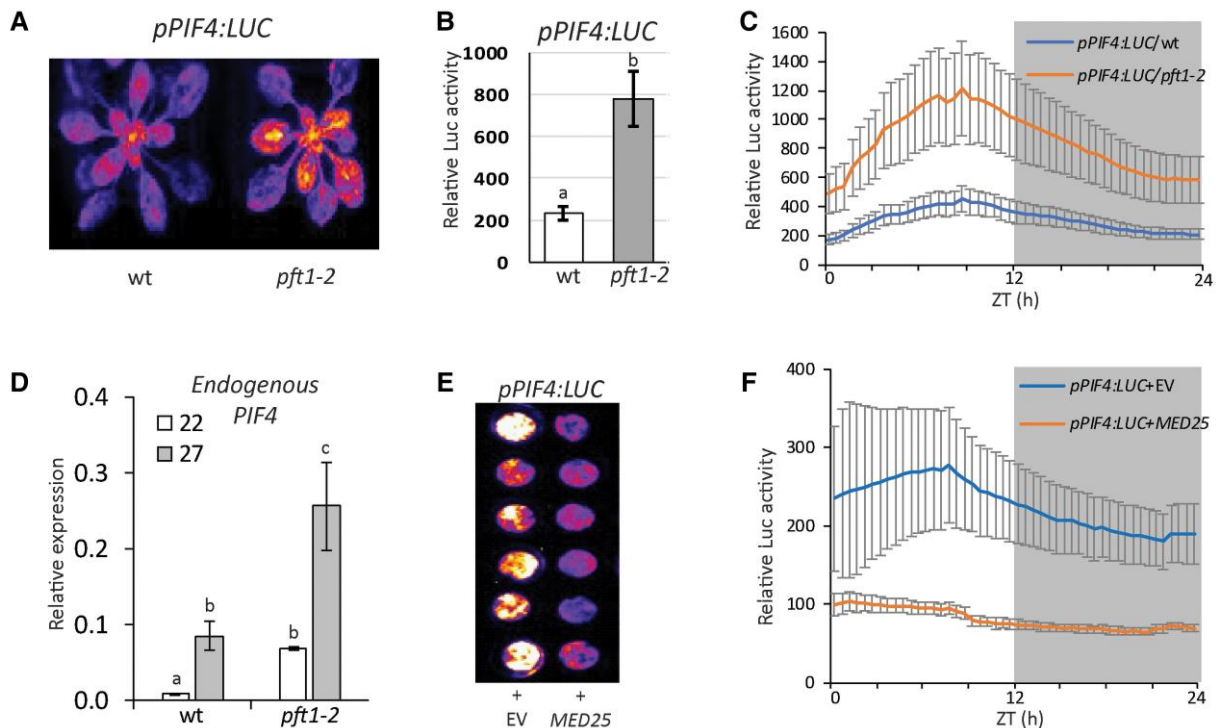


Figure 2 MED25 limits *PIF4* expression. **A**, *pPIF4:LUC* activity imaged in 3-week-old WT and *pft1-2* plants. **B**, Quantification of *pPIF4:LUC* activity in 2-week-old WT and *pft1-2* plants. The data represent the mean \pm SE ($n = 5$ seedlings). Different small letters indicate a significant difference as calculated by a student *T*-test ($P < 0.05$). The experiment was repeated multiple times (with plants at different ages) with similar results. **C**, Quantified diurnal *pPIF4:LUC* activity in 3-week-old WT and *pft1-2* seedlings under 12 h light/12 h darkness of ZT. Error bars represent mean \pm SE. **D**, Endogenous *PIF4* expression in 2-week-old WT and *pft1-2* seedlings at 22°C and 27°C. Sampling was at ZT = 8 h, near the peak of *PIF4* expression. The data represent the mean \pm SE of three replicate samples containing at least 15 seedlings. Quantification was done by RT-qPCR using *PIF4*-specific primers. Different small letters indicate a significant difference as calculated by a student *T*-test ($P < 0.05$). **E**, *In planta pPIF4:LUC* activity in transient expression assay with EV; left) or in the presence of 35S:*MED25* (right) at 3 days post-agroinfiltration. **F**, Quantification of *pPIF4:LUC* activity in six independent leaf disc from transient expression assay (shown in Figure 2E) over a 12 h light/12 h darkness of zeitgeber time (ZT). The LUC activity in an interval of 5 min is monitored in these leaf discs every half hour. Error bars represent mean \pm SE ($n = 6$ leaf disc).

opposite (at 27°C), indicating that the action of *PIF4* in hypocotyl elongation response requires *MED25*.

MED25 stimulates expression of *YUCCA8* at 27°C

Since elongation growth responses are tightly linked with increased expression of auxin biosynthesis genes like the *PIF4* target gene *YUCCA8* (Koini et al., 2009; Sun et al., 2012), we subsequently investigated the effect of *MED25* on *YUCCA8* expression. Expression of *YUCCA8* was quantified at ZT = 8 h in 2-week-old WT and *pft1-2* seedlings grown at 22°C or 27°C. Results show that the expression of *YUCCA8* is similar in WT and *pft1-2* at 22°C (Figure 3A), despite the higher *PIF4* expression in *pft1-2* at 22°C (Figure 2). As expected, high temperature (27°C) led to significantly increased expression of *YUCCA8* in WT (Figure 3A) (Koini et al., 2009; Sun et al., 2012). But this effect was limited in the *pft1-2* mutant background (Figure 3A), where again we also recorded a higher expression of *PIF4* at 27°C (Figure 2).

The effect of *MED25* on *YUCCA8* expression was next tested in a transient expression assay at 22°C in *N.*

benthamiana leaves, using a *pYUCCA8:LUC*-reporter and 35S:*PIF4* and 35S:*MED25* effector constructs. The relative *pYUCCA8:LUC* activity was quantified in extracts of infiltrated leaves and normalized to the activity of a co-infiltrated 35S:*Renilla:LUC*-reporter construct. Results show that, in contrast to the effect of *MED25* on *PIF4* expression in Arabidopsis (Figure 2, E and F), the basal activity of *pYUCCA8:LUC* in *N. benthamiana* leaves is not affected by *MED25* (Figure 3B). When *pYUCCA8:LUC* was however co-infiltrated with the 35S:*PIF4* effector construct, the relative expression from the *YUCCA8* promoter was increased as expected (Oh et al., 2012). We also observed that *MED25* did not affect the *PIF4* effect on *pYUCCA8:LUC* expression (Figure 3B). Thus, the effect of *MED25* on endogenous *YUCCA8* expression in Arabidopsis cannot be reconstituted in a transient expression assay in *N. benthamiana*.

Overall, our results hint to dual, but seemingly opposite roles, for *MED25* in thermomorphogenesis responses in Arabidopsis. First, *MED25* inhibits the expression of *PIF4* at normal and elevated temperatures, but at the same time,

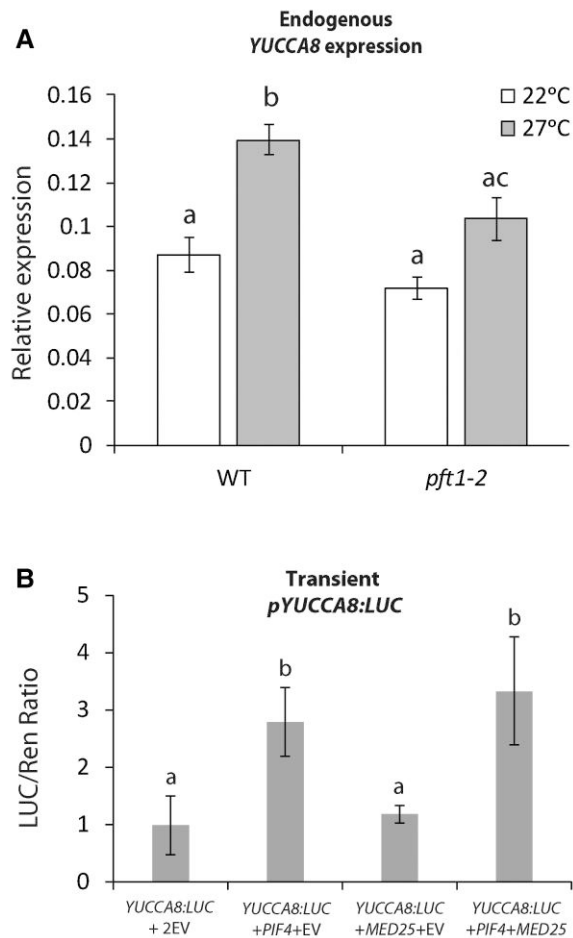


Figure 3 MED25 promotes the expression of YUCCA8 at warm temperatures. A, Endogenous (relative) YUCCA8 expression in 2-week-old WT and *pft1-2* mutant seedlings as quantified by RT-qPCR (pooled seedlings, technical replicates $n = 3$) Error bars represent mean \pm SD. Different small letters indicate a significant difference as calculated by a student *T*-test ($P < 0.05$). B, *pYUCCA8:LUC* activity in transient expression assays. Leaves were infiltrated with reporter *pYUCCA8:LUC* with effector constructs EV, 35S:*PIF4*, 35S:*MED25*, or combinations thereof. LUC activity was monitored in at least eight leaf discs from independent infiltrated leaf areas. The data represent the mean \pm SE ($n = 8$). Different small letters indicate a significant difference as calculated by a student *T*-test ($P < 0.05$).

MED25 seems required for full induction of the PIF4 target gene YUCCA8 at elevated temperatures. It is noted that MED25 is a member of the Mediator multiprotein complex and, therefore, while loss of MED25 in the *pft1* mutants equates to fewer complete intact Mediator complexes that include MED25, overexpression of MED25 may not necessarily produce more copies of the Mediator complex and therefore, more MED25-dependent mediator action. However, there are examples of MED25 overexpression exerting effects as seen in this study, but which may be the result of MED25 acting independently of the complex (Xu and Li, 2011).

MED25 protein can bind to PIF4 in *in planta*

We show that Arabidopsis MED25 limits the transcriptional activity of PIF4 but stimulates the expression of the PIF4 target gene YUCCA8 at warm temperatures. Since PIF4 can bind to its own promoter (Chow et al., 2019), we hypothesized that MED25 may influence the transcriptional activity of PIF4 at the PIF4 promoter. Indeed, several potential PIF4 binding sites were detected at the PIF4 and YUCCA8 promoters (Supplemental Table 1). Although PIF4 was not identified as interactor of MED25 in Arabidopsis using a yeast-2-hybrid assay (Ou et al., 2011), it was shown that tomato MED25 interacts with tomato PIF4 (Sun et al., 2020). We, therefore, decided to test the putative interaction between Arabidopsis PIF4 and MED25 using *in planta* BiFC and split-luciferase binding assays (Chen et al., 2008).

For the BiFC assay, *Agrobacterium* cells carrying either *nYFP-PIF4*, *MED25-cYFP*, or *mCherry* with nuclear localization signal (*mCherry*^{NLS}), were co-infiltrated into *N. benthamiana* leaves. *nYFP-6xmyc* and *6xmyc-cYFP* constructs were used as a negative control. At 3 days post-agroinfiltration, reconstituted yellow fluorescent protein (YFP) activity was observed in the nucleus where it also colocalized with the mCherry signal (Figure 4A). This indicates that PIF4 interacts with MED25 protein in the nucleus. The interaction between MED25 and PIF4 was subsequently tested by Co-IP in Arabidopsis plants expressing either immuno-tagged MED25 (35S:*MED25-myc*) and/or tagged PIF4 protein (35S:*PIF4-HA*). Results show that MED25 protein can be detected in the protein fraction isolated from the double-tagged line using antibodies against the HA-tagged PIF4 protein (Figure 4B), indicating that MED25 associates with PIF4 in Arabidopsis seedlings.

For the split-luciferase assay, expression constructs of MED25 with an N-part of LUC (35S:*MED25-nLUC*) and the expression construct of PIF4 with an N-terminal fusion with cLUC (*PIF4-cLUC*) were developed and introduced into *Agrobacterium*. Different combinations of the split-LUC fusion proteins were co-expressed in *N. benthamiana* leaves by co-agroinfiltration and at 3 days post-agroinfiltration the *in planta* LUC activity was imaged and quantified. Results show that the co-expression of *MED25-nLUC* with *PIF4-cLUC* results in a reconstitution of luciferase activity, again indicating an effective and direct interaction between MED25 and PIF4 proteins *in planta* (Figure 4C) in line with luciferase binding assays that have been used to demonstrate the interaction of MED25 with TCP or COI1 (An et al., 2017; Liu et al., 2017).

The MED25 protein contains multiple domains, each with specific functions: the von Willebrand Factor A domain (vWF-A), middle domain (MD), acidic acid domain (ACID), and poly glutamine (Q) track (GD) (Supplemental Figure 2). The GD domain contains glutamine repeats called the polyQ tract (Cerdan and Chory, 2003; Backstrom et al., 2007; Elfving et al., 2011; Inigo, Giraldez, et al., 2012; Rival et al., 2014). These different subdomains of MED25 were cloned separately, each provided with an ATG start codon

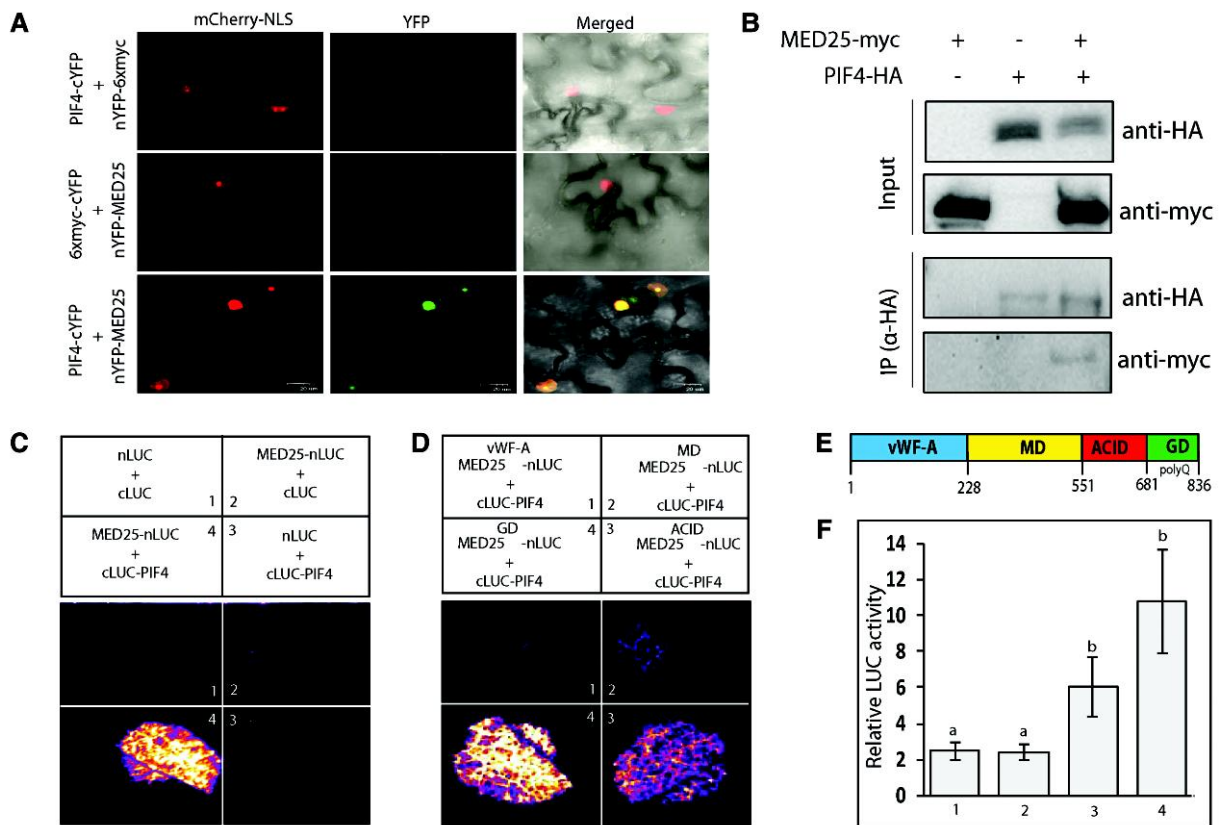


Figure 4 MED25 interacts with PIF4 *in planta*. A, BiFC assay in *N. benthamiana* leaves. cYFP was fused to full-length PIF4 and nYFP was fused to full-length MED25. mCherry^{NLS} marks the nucleus. 6xmyc with cYFP or nYFP was used as negative control, respectively. Confocal images were taken at 3 days post-agroinfiltration. Scale bar 20 mm B, Co-immunoprecipitation (IP) shows that PIF4 binds to MED25 in Arabidopsis. Protein extracts derived from 10 days old transgenic 35S:PIF4-HA, 35S:MED25myc, and F1 (35S:PIF4 35S:MED25myc) plants were immunoprecipitated for 2 h using anti-HA Magnetic Beads. The input and immunoprecipitated products were detected by anti-HA monoclonal and anti-myc polyclonal antibodies by western blot. C, Split-LUC assays showing specific interaction between cLUC-PIF4 and MED25-nLUC. The design of the co-infiltrations is shown on top. D, split-LUC assays from specific interaction between cLUC-PIF4 and MED25 subdomains MED25^{GD}-nLUC and MED25^{ACID}-nLUC. Expression constructs encoding MED25 subdomains fused to nLUC were co-infiltrated with expression construct encoding PIF4-cLUC. In each experiment, the relative gene dosage of cLUC and nLUC constructs was kept constant. A single representative LUC activity image was taken of all discs at 3 days post-agroinfiltration. Shown are selected discs from each infiltration, digitally cut from a single LUC activity image. E, Schematic structure of the MED25 protein with the four subdomains and their AA position along the protein sequence: vWF-A, MD, ACID, and the PolyQ-containing GD. F, Quantification of reconstituted split-LUC activity from the interaction between cLUC-PIF4 and nLUC fusions with each of the four different MED25 domains (for samples see panel D)). The data represent the mean ± SE ($n = 5$). Different small letters indicate a significant difference as calculated by a student *T*-test ($P < 0.05$).

and at the C-terminus fused *in-frame* to the nLUC sequence in expression constructs (vWF-A-nLUC; MD-nLUC; ACID-nLUC and GD-nLUC). The interaction of PIF4 with each of these MED25 subdomains was tested in transient expression assays and LUC activity was imaged in infiltrated leaves at 3 days post-agroinfiltration. Results show that PIF4 mainly interacts with the GD and Acid domains of MED25 (Figure 4, D–F).

Interaction of MED25 with the PIF4 and YUCCA8 loci increases at warm temperatures

Since MED25 affects the expression of PIF4 and YUCCA8, subsequently, the ability of MED25 to associate with the

PIF4 and YUCCA8 loci was tested by chromatin-immunoprecipitation (ChIP) assays using 3-day-old seedlings grown at either 22°C or 27°C. To this aim, we generated transgenic plants that overexpressed C-terminal HIS-tagged MED25. Col-0 plants were included as negative control. At 22°C, limited binding of MED25 to the PIF4 promoter and exon was detected, as the signal was in the same range of that of the negative control (Figure 5A). However, the signal increased substantially in 27°C-grown plants, for both MED25 binding to the PIF4 promoter and to the PIF4 exon region (Figure 5A). In contrast to PIF4, binding of MED25 was detected at different positions at the YUCCA8 locus already at 22°C. Overall, MED25 association to the YUCCA8 locus also increased at high temperatures

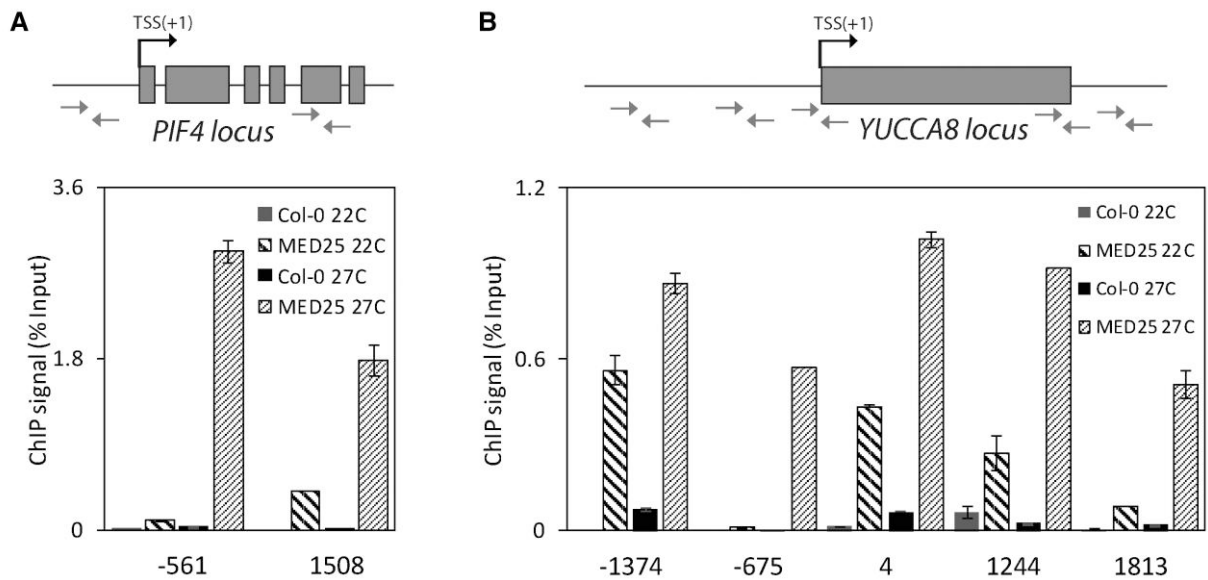


Figure 5 MED25 association to the *PIF4* and *YUCA8* loci increases at warm temperature. A and B, Relative ChIP-qPCR signal of MED25 at the *PIF4* (A) and *YUCA8* (B) loci, at DNA regions indicated in the schematics above the graphs, at 22°C and 27°C. Col-0 was used as negative control for both temperatures. Black arrows and position +1 depict the transcription start site (TSS). Gray boxes indicate exons. Small gray arrows indicate the position of the primers used for ChIP qPCR along the loci (Zhu et al., 2016). Bars are means \pm SE ($n = 4$). Table S2 lists the putative *PIF4* binding sites at the *PIF4* and *YUCA8* promoter according to Plant Pan 3.0 (Chow et al., 2019).

(Figure 5B). These results indicate that high temperature leads to an increase of MED25 binding to *PIF4* and *YUCA8*. Increased MED25 binding at *PIF4* and *YUCA8* loci could also be due to higher transcriptional activity related to warm temperature. Apparently, the full expression of *YUCA8* requires both *PIF4* and MED25, as increased *PIF4* expression in the *pft1-2* mutant does not coincide with increased *YUCA8* expression (Figures 2 and 3). Results thus support the hypothesis that MED25 may be required for *PIF4* transcriptional activity at the *YUCA8* locus at warm temperatures.

HDA9 binds to MED25 but not to PIF4 in planta

Our results so far indicate that MED25 is required for proper hypocotyl elongation in response to high temperatures. Similarly, the histone-modifying enzyme HDA9 is required for this thermomorphogenesis response and for transcriptional induction of *YUCA8* (van der Woude et al., 2019). We tested the genetic interaction between MED25 and HDA9 using a *pft1-2 hda9-1* double mutant and quantified hypocotyl elongation in the respective single and double mutants at 22°C and 27°C. Results show that the *hda9-1* mutation does not further suppress the already reduced hypocotyl elongation by the *pft1-2* mutation (Figure 6A), hinting to the possibility that MED25 and HDA9 might work together in the same pathway toward hypocotyl elongation.

It is not clear how HDA9 is recruited to the *YUCA8* locus during thermomorphogenesis (van der Woude et al., 2019). We hypothesized that MED25 may be involved, and we investigated this by testing whether MED25 can interact with HDA9,

using Y2H, BiFC, and split-luciferase assays. Indeed, in the yeast-two-hybrid assays an interaction between HDA9 and MED25 proteins was detected (Figure 6B). For the BiFC assay, *HDA9* and *MED25* CDS sequences were fused to N-terminal and C-terminal of *YFP*, respectively. Co-expression of these fusion constructs reconstituted *YFP* activity in the nucleus of co-infiltrated *N. benthamiana* leaves, based on co-localization of the *YFP* signal with the nuclear mCherry signal (Figure 6C), confirming the interaction between HDA9 and MED25. For the split-LUC assay, an expression construct encoding *cLUC-HDA9* was made and co-infiltrated with *MED25-nLUC*. The co-expression resulted in a strong luminescence signal, further confirming that MED25 can indeed interact with HDA9 in planta (Figure 6, D and E). By contrast, co-infiltration of expression constructs encoding *PIF4-nLUC* and *cLUC-HDA9* fusion proteins did not result in substantial reconstitution of LUC activity (Figure 6, D and E), corroborating our previous finding (van der Woude et al., 2019) that HDA9 does not directly interact with *PIF4*. Reconstituted split-LUC activity by interaction between MED25 + *PIF4* or MED25 + HDA9 is not additive upon co-expression of MED25 + *PIF4* + HDA9 (Supplemental Figure 3). MED25 subdomain mapping with split-LUC assays revealed that the MED25–HDA9 interaction is mainly explained by interaction between the GD domain of MED25, and less so between HDA9 and the MED25 ACID and MD subdomains (Figure 6, F and G).

MED25 affects HDA9-LUC activity

Previous work indicated that HDA9 protein is likely stabilized in young seedlings in response to warm temperatures

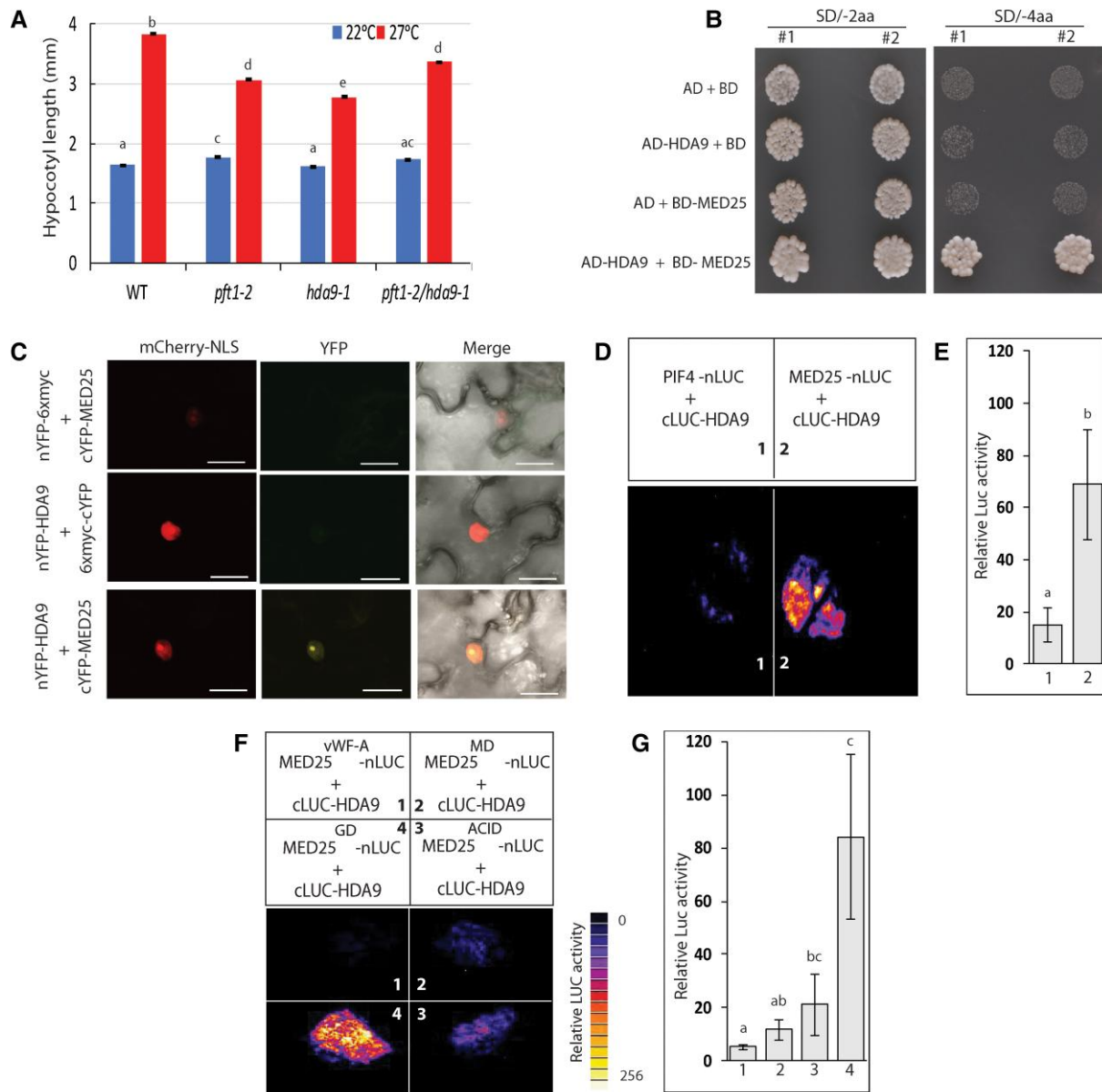


Figure 6 MED25 interacts with HDA9. **A**, Hypocotyl length assay of *hda9-1* and *pft1-2* mutants and their double mutant combination. Average Arabidopsis hypocotyl length with st. error bars ($N = 46$ seedlings). Plants were grown for 7 days after germination at 22°C or 27°C in 8 h light/6 dark, under mixed (R, B, F) LED lights. Different letters indicate significant differences as calculated by a Tukey HSD post hoc test ($P < 0.001$). **B**, Y2H assay showing HDA9 interaction with MED25 in yeast. Yeast transformants were plated on SD medium lacking Leu and Trp amino acids (–2aa) and SD medium lacking His, Ade, Leu, and Trp amino acids (–4aa). All plates were incubated at 30°C for 3 days. **C**, BiFC assay showing HDA9 and MED25 protein interaction in the nucleus. nYFP-HDA9 and MED25-cYFP constructs were premixed with mCherry^{NLS} and co-infiltrated into *N. benthamiana* leaves. Confocal image was taken at 3 days post-agroinfiltration. **D**, Split-LUC assays indicating that HDA9 physically interacts with MED25, but not PIF4. The design of the co-infiltrations is shown above the images. A single LUC activity image was taken of all discs at 3 days post-agroinfiltration. Shown are selected discs from each infiltration, digitally cut from single LUC activity image. **E**, Quantification of relative LUC activity of HDA9-PIF4 and HDA9-MED25 split-LUC interactions indicated in (D). The data represents the mean \pm SE ($n = 6$). Different small letters indicate a significant difference as calculated by a student *T*-test ($P < 0.05$). **F**, HDA9 interacts most strongly with the GD domain of MED25. The design of the co-infiltrations is shown on top. Added to legend: A single LUC activity image was taken of all discs at 3 days post-agroinfiltration. Shown are selected discs from each infiltration, digitally cut from single LUC activity image. **G**, Quantification of relative LUC activity of HDA9 and MED25 subdomains interaction in split-LUC interactions indicated in Added to legend: A single LUC activity image was taken of all discs at 3 days post-agroinfiltration. Shown are selected discs from each infiltration, digitally cut from single LUC activity image (F). The data represent the mean \pm SE ($n = 6$). Different letters indicate significant differences as calculated by a student *T*-test ($P < 0.05$).

and this stabilization is proposed to trigger histone deacetylation events required for H2A.Z eviction and subsequent *YUCCA8* transcriptional activation by PIF4 (van der Woude et al., 2019). Since MED25 interacts with HDA9 at the protein level, we investigated whether this interaction affects HDA9 protein stability. To this aim, a fusion between HDA9 protein and luciferase was expressed under control of the constitutive 35S promoter (*35S:HDA9-LUC*) (van der Woude et al., 2019). The construct was first introduced into the WT background and subsequently crossed into the *pft1-2* mutant background and into a *MED25* overexpression line (*35S:MED25*). By crossing into the tested backgrounds, a potential genomic position effect (Matzke and Matzke, 1998) on LUC activity is excluded. HDA9-LUC activity was measured in 7-day-old homozygous seedling in the LUMINATOR setup under diurnal 12 h light/12 h darkness conditions at 22°C. The second day, temperature was

switched to 28°C 3 h after the start of the photoperiod (Figure 7).

Quantification of the HDA9-LUC signal reveals a striking increase of HDA9-LUC activity during the night. Interestingly, in the *pft1-2* background, the average *had9-LUC* activity was consistently higher than in WT, indicating that the stabilization of HDA9 is antagonized by MED25 (Figure 7A). This was confirmed by testing a line that overexpressed MED25, wherein we observed the opposite, namely a severely suppressed HDA9-LUC activity. At 27°C in the light, the LUC activity was slightly higher than at 22°C, while at 27°C during the night LUC activity was almost threefold higher than at 22°C in the dark in the wild type (Figure 7B). Control experiments show that transcription from *35S:HDA9-LUC* constructs is higher at 27°C than at 22°C (Supplemental Figure 4A). Taking this into account, it cannot fully be excluded that higher LUC activity during

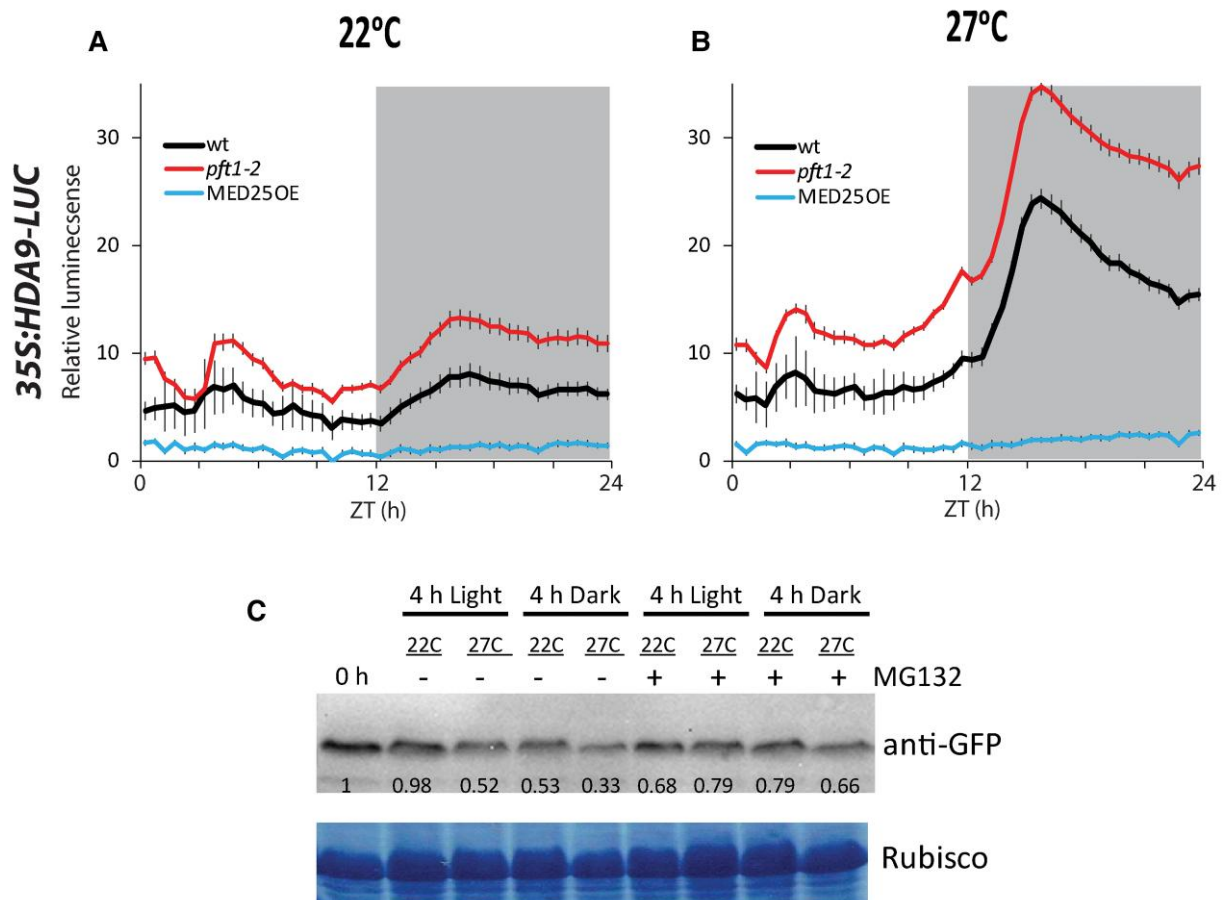


Figure 7 HDA9-LUC stability is affected by MED25. Seeds of *35S:HDA9-LUC*-reporter lines in the WT (bla, *pft1-2*, and *35S:MED25* (*MED25OE*) backgrounds were stratified and germinated in growth cabinets under diurnal fluorescent white light (12 h light/12 h darkness). At 6 days after germination plants were sprayed with substrate luciferin (1 mM) and placed in the LUMINATOR setup. A, *35S:HDA9-LUC* in WT (black line), *pft1-2* (red line), and *35S:MED25* (blue line) under 12 h light/12 h darkness of zeitgeber time (ZT) and constant 22°C and (B) at 27°C. At least 18 seedlings were tested for each reporter line. Error bars represent mean \pm SE. C, In a separate reporter line, eGFP-HDA9 protein levels were measured in seedlings expressing *35S:eGFP-HDA9* at 4 h in light and at 4 h in darkness at 22°C or 27°C. Intensity of the band detected by anti-GFP is quantified relative to protein level at T = 0. Loading was normalized to Rubisco staining on the blot. The experiment was done in the absence (–) or presence (+) of the proteasome inhibitor MG132.

warmth is, at least in part, explained by increased transcription at 27°C. Transcript levels from 35S:HDA9-LUC is highest in the MED25 OE background (Supplemental Figure 4A), while LUC activity is very low in this line (Figure 7B). This confirms the destabilization effect by the ectopic high MED25 levels on the HDA9-LUC fusion protein in these plants. The observed differences in transcription levels from 35S:HDA9-LUC in the WT, *pft1-2*, and MED25 OE lines (Supplemental Figure 4A) could be an indication that MED25 also affects transcription from the exogenous 35S promoter. It also cannot be excluded that the observed increase in 35S-HDA9-LUC activity at 27 degrees results from a temperature effect on LUC enzymatic activity. However, the effect of temperature on 35S:LUC activity is less extreme than observed for 35S:HDA9-LUC plants (Supplemental Figure 4B). While endogenous MED25 contributes to the destabilization of HDA9-LUC protein in the light, the relative increase of HDA9-LUC activity in the dark is similar at 22°C and 27°C. This suggests that in the dark MED25 has no further effect on HDA9-LUC (Figure 7, A and B). The fact that HDA9-LUC protein stability is seemingly negatively regulated by ectopic high expression of MED25 may explain why plants overexpressing MED25 show a phenotype similar to the *pft1-2* and *hda9-1* mutant (Figures 1B and 6A). While HDA9 protein is more stable at 27°C in the presence of low endogenous MED25 levels, in the presence of high ectopic MED25 protein levels, the destabilizing effect of MED25 on HDA9 protein stability (Figure 7). Western blot analysis was used to test for HDA9-GFP fusion protein levels at the two different temperatures. Results show a decrease rather than an increase of eGFP-HDA9 protein level at elevated temperatures, both in light and in dark (Figure 7C). The fusion protein levels were also tested in presence of the proteasome inhibitor MG132, which resulted in increased eGFP-HDA9 protein levels at elevated temperature, both in light and in dark (Figure 7C), confirming previous results indicating that HDA9 is affected by proteasome activity (Mayer et al., 2019). The experiment was repeated with similar results (Supplemental Figure 5).

Discussion

MED25 forms a potential link between PIF4 and HDA9 at the YUCCA8 locus

The hypocotyl elongation response of Arabidopsis seedlings under warm temperature conditions is mediated by many different transcription factors and phytohormone biosynthesis and signaling pathways (reviewed in (Casal and Balasubramanian, 2019)). Thermomorphogenesis responses also involve epigenetic processes (Perrella et al., 2022). Among the most notable are the epigenetic changes occurring at the YUCCA8 locus, via the action of PWR and HDA9. These factors trigger a net eviction of H2A.Z-containing histones from the YUCCA8 locus, allowing access to transcription factors, like PIF4 (Tasset et al., 2018; van der Woude et al., 2019). PIF4-mediated induction of YUCCA8

then results in a higher auxin biosynthesis capacity, which triggers the elongation response (Bellstaedt et al., 2019).

Despite the known PIF4 association to the YUCCA8 genomic region (Franklin et al., 2011; Sun et al., 2012), so far it was not clear how HDA9 is specifically recruited to this locus under warmth (van der Woude et al., 2019). Our research provides evidence that a specific component of the Mediator complex, MED25, can bind to both PIF4 and HDA9 (Figures 4 and 6) and associates to the YUCCA8 locus mainly at 27°C (Figure 5). Accordingly, MED25 is required for YUCCA8 induction at high temperatures (Figure 3) and thermomorphogenesis (Figure 1).

The amino terminus of MED25 has a conserved von Willebrand Factor Type A (vWF-A) domain, which mediates the interaction between MED25 and the Mediator complex via binding with the subunit MED16 (Yang et al., 2014) (Supplemental Figure 2). The vWF-A domain also interacts with MBR1 and MBR2, which are involved in the degradation of MED25 (Inigo, Giraldez, et al., 2012). Transcription factors such as AP2/ERF and MYCs and suppressors such as JAZ proteins interact with the ACID (activator interacting domain) domain of MED25 (Supplemental Figure 2). At the C-terminus, MED25 has a conserved glutamine rich (*polyQ*) tract, named GD domain, and it has been speculated that this domain is involved in transcriptional activation (Cerdan and Chory, 2003; Backstrom et al., 2007; Elfving et al., 2011). Moreover, the length of this *polyQ*-rich region affects MED25-mediated flowering (Rival et al., 2014). Our interaction studies of different MED25 subdomains with PIF4 and HDA9 (Supplemental Figure 2) indicate that PIF4 can interact with the ACID and GD domain (Figure 4), while HDA9 interacts mainly with the GD domain (Figure 6). In tomato, in the context of the shade-induced elongation responses, an interaction between the tomato MED25 and the homolog of PIF4 has also been demonstrated (Sun et al., 2020). Although both PIF4 and HDA9 interact with the GD domain of MED25, this interaction may not be mutually exclusive. Indeed, when HDA9 was co-expressed with MED25 and PIF4 in the split-LUC assays, the reconstituted luciferase activity is equal to or larger than that of reconstituted luciferase by the MED25 + PIF4 interaction alone (one example shown in Supplemental Figure 3). The fact that PIF4 can bind to target loci, while MED25 can interact both with PIF4 and HDA9 suggests that MED25 plays a role in recruiting HDA9 to PIF4 target loci.

Are other transcription factors also involved in recruiting HDA9 to YUCCA8 locus?

In Arabidopsis, loss of either HDA9 or MED25 results in a reduced hypocotyl elongation response, with no additive effect for hypocotyl elongation in the *pft1-2 hda9-1* double mutant (Figure 6). This could suggest that HDA9 and MED25 function in the same pathway toward high-temperature-induced elongation. Besides PIF4, transcription factor BZR1 is also limiting for the high-temperature-induced expression of YUCCA8 (Bai et al., 2012; Oh et al., 2012). We found evidence for interaction between MED25 and BZR1 using our

split-LUC assay (Supplemental Figure 6). Therefore, we speculate that even in the absence of PIF4, HDA9 may still be recruited to the *YUCCA8* locus via BZR1 and MED25. Activation of *YUCCA8* at 27°C is also associated with histone deacetylation (van der Woude et al., 2019). The transcription regulator SEUSS (SEU) was shown to affect H3K4me3 methylation at loci of growth-stimulating genes (Huai et al., 2018). SEU can interact with PIF4 protein only at elevated temperatures, because at normal temperatures both SEU and PIF4 are destabilized through their interaction with PHYB (Huai et al., 2018). On the other hand (changes in) histone acetylation levels at the *YUCCA8* locus at 27°C are dependent on HDA9, but not on PIF4, as *pij4-2* mutant at 27°C displays similar H3K9K14AC levels compared to the wild type (van der Woude et al., 2019). Like HDA9, the transcriptional regulator SEU may therefore be recruited to *YUCCA8* by other factors besides PIF4. Interestingly, the homolog of SEU in Arabidopsis, LEUNIG, has been shown to interact with MED25 in the context of MYC2-dependent transcriptional activation (You et al., 2019). Future research will need to show how and when all these different factors can interact and are recruited to affect growth-regulating genes during thermomorphogenesis.

MED25 functions differently at the PIF4 locus compared to the YUCCA8 locus

While the action of MED25 at the *YUCCA8* locus is required for full activation of transcription at elevated temperatures, MED25 seemingly limits *PIF4* transcription, both at 22°C and at 27°C, as demonstrated by the *PIF4:LUC* reporter and by qPCR, testing endogenous *PIF4* expression in WT and *pft1-2* (Figure 2). Our ChIP-qPCR experiments however indicate that unlike at the *YUCCA8* locus, at the *PIF4* locus the association with MED25 protein increases at elevated temperatures (Figure 5). Figure 8, A and B, shows a putative model for the role of MED25 in the expression of *PIF4*. At 22°C MED25 is limiting expression of *PIF4*. At present, it is not clear how this is achieved, but two alternatives are proposed (indicated as 1 and 2 in the figure). The high-temperature-induced expression of *PIF4* is associated with reduced H3K9 acetylation levels at the +1 nucleosome of *PIF4* (Tasset et al., 2018). Although it was suggested that POWERDRESS (PWR), an interacting partner of HISTONE DEACETYLASE 9 (HDA9), is required for H3K9 deacetylation at the *PIF4* locus, HDA9 itself has no substantial effect on *PIF4* transcription at neither control nor warm temperatures (van der Woude et al., 2019). Hence, epigenetic control of *PIF4* expression is, at least for a large part, HDA9 independent, suggesting that other HDACs rather than HDA9 may have a role. Also, at 27°C MED25 is limiting expression of *PIF4*. MED25 may regulate *PIF4* expression directly by regulating *PIF4* locus accessibility through recruitment of HDACs, other than HDA9, at both 22°C and 27°C (indicated by HDA? in Figure 8). Alternatively, MED25 may affect *PIF4* expression indirectly, by affecting the recruitment of transcription factors (TFs) effectively responsible for *PIF4*

expression, or by affecting co-factor activity for these TFs, both at 22°C and 27°C. The overall effect of MED25 would thus be reduced *PIF4* transcription. One likely candidate for this MED25-dependent recruitment to the *PIF4* locus could be BZR1 but could also involve PIF4 itself through binding of PIF4 to its own promoter. In addition, TEOSINTE BRANCHED 1/CYCLOIDEA/PCF (TCP) transcription factors TCP5, TCP13, and TCP17 could be involved, as they are required for elongation responses and elevated expression of *PIF4* at 27°C (Zhou et al., 2019). For TCP17 it has been shown that it interacts with PIF4 (Zhou et al., 2019). Although an interaction between TCP17 and MED25 has not been demonstrated, it has been shown that MED25 interacts with TCP4 in the context of the regulation of flowering (Liu et al., 2017). An increased association of TCP4 and MED25 at the promoter region of flowering gene *CONSTANS* (*CO*) is related to enhanced *CO* transcription and induction of flowering (Yao et al., 2019), while MED25 was found to associate with the promoter region of *CO*, which is also occupied by TCP4 (Liu et al., 2017).

The LUC signal intensities of *35S:HDA9-LUC* in established (7 days old) seedlings and 3 weeks old plants do not show a strong increase in LUC activity at the onset of light at elevated temperature as it was observed in 3-day-old seedlings (van der Woude et al., 2019), while the total HDA9-LUC protein levels do not show a strong increase at elevated temperature in older plants (Figure 7). Therefore, activation of the elongation response by HDA9 activity at high temperatures is not due to the stabilization of HDA9 protein in older plants, but rather may be explained by regulation of nuclear HDA9 levels at elevated temperature (Mayer et al., 2019).

Figure 8, C and D shows a putative model for the role of MED25 in regulating expression of *YUCCA8*. At 22°C, binding of BZR1 to the *PIF4* locus may be limited due to (among others) low BR signaling and low BZR1 nuclear import (Ibanez et al., 2018). Accessibility for PIF4 and MED25 to the chromatin of the *YUCCA8* locus is limited by high levels of repressive H2A.Z histone occupancy in these conditions (van der Woude et al., 2019). In addition, at 22°C, the binding of co-activator SEU and histone-modifying enzymes (HME) to chromatin of auxin biosynthesis genes like *YUCCA8* is also limited (Huai et al., 2018). Possibly, access to the *YUCCA8* locus at 22°C is also limited for BZR1 (Ibanez et al., 2018). At 27°C, nuclear import of BZR1 is increased, resulting in increased expression of *PIF4* (Ibanez et al., 2018). While in established seedlings (8 days old) HDA9 protein levels are similar at 22°C and 27°C degrees (Figure 7), nuclear HDA9 activity or HDA9 post-transcriptional modification may be increased at elevated temperatures (Mayer et al., 2019), thereby influencing HDA9 recruitment over *YUCCA8* locus, possibly via interaction with MED25. Increased HDA9 activity at the *YUCCA8* locus triggers local H3K9K14ac deacetylation. This results in net low levels of H2A.Z at *YUCCA8*, proposedly because H2A.Z incorporation is less efficient (van der Woude et al., 2019). HDA9 does not directly interact with PIF4 in split-LUC (this study) and Y2H

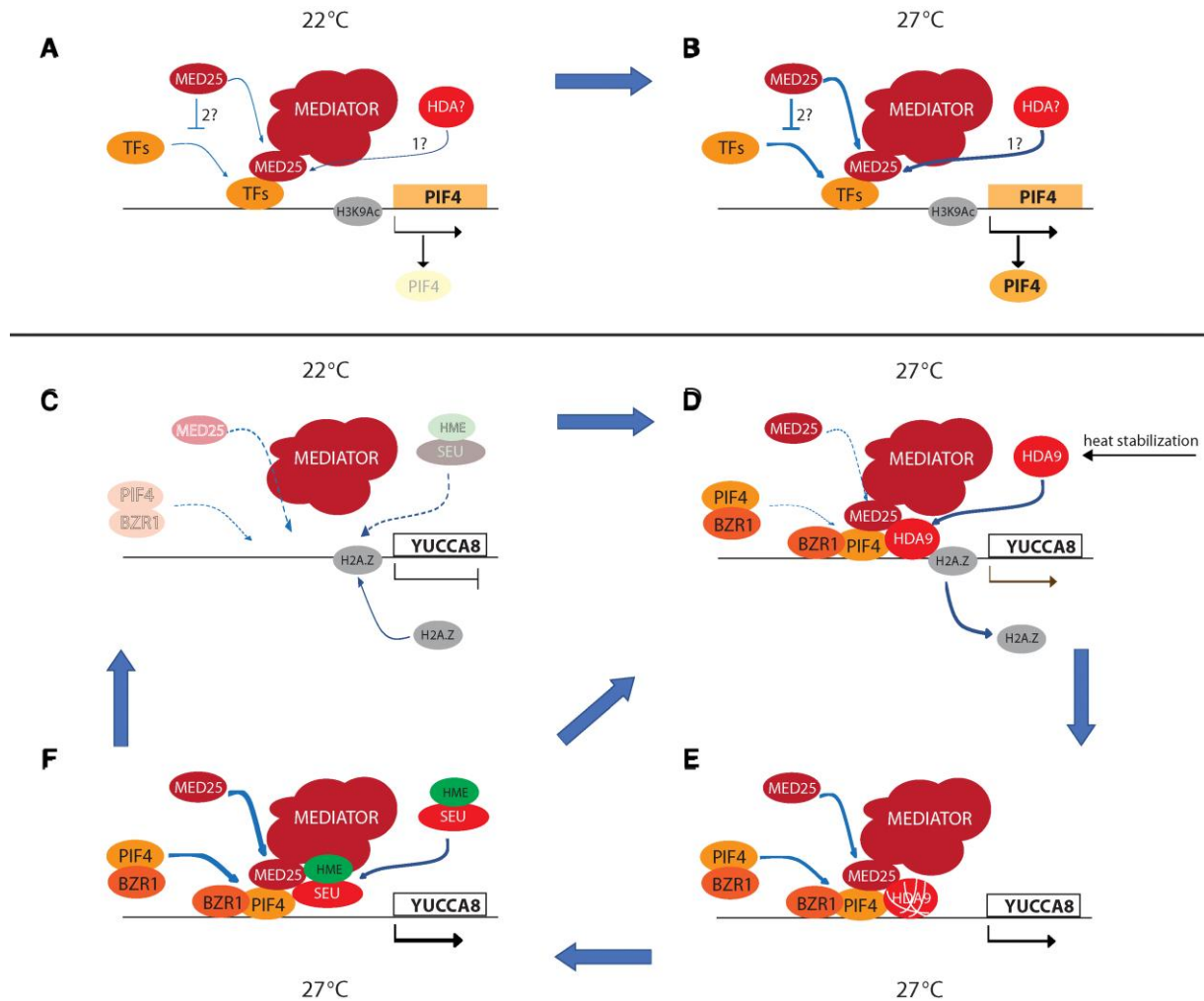


Figure 8 Proposed model of the roles of MED25 during thermomorphogenesis. A and B, At both control and elevated temperatures the increase in transcriptional output of *PIF4* is limited by MED25. C–F, By contrast, at elevated temperatures, MED25 stimulates expression of *YUCCA8*, presumably by recruiting HDA9 through binding of MED25 to PIF4 and binding of HDA9 to MED25. Nuclear HDA9 protein activity may be increased at elevated temperatures (Mayer et al., 2019). The action of HDA9 activity at the *YUCCA8* locus is limited by the destabilization of HDA9 protein through the interaction with MED25 and histone re-acetylation activity upon return to normal temperature. For further details see text. Dashed arrows: very weak interaction; Lines with blunt end: negative interaction. Thin/thick arrows: weak/strong interaction. Dashed arrows: very weak interaction. Very thick arrows between subfigures indicate progression complex formation at the locus.

and BiFC (van der Woude et al., 2019) assays and deacetylation at the *YUCCA8* locus still occur in *pif4* mutant. This indicates that HDA9 recruitment to *YUCCA8* is not dependent on PIF4 and that other transcription factors/DNA-binding proteins acting at the *YUCCA8* locus are likely involved (e.g. BZR1, which also interacts with MED25: Supplemental Figure 6). Increased binding of BZR1 over the *YUCCA8* locus at 27°C has been demonstrated (Ibanez et al., 2018). The net depletion of histone H2A.Z from the *YUCCA8* chromatin at 27°C allows the increased frequency of binding of PIF4 and possibly also BZR1 and MED25, while HDA9 protein is proposedly sequestered (inactivated) by its interaction with MED25 (Figure 7). At 27°C, PIF4 at the *YUCCA8* locus interacts with the scaffolding protein co-activator SEU, which is required to stimulate the expression of *YUCCA8*

(Huai et al., 2018). BZR1 has also been implemented in modulating *YUCCA8* levels (Oh et al., 2012). Therefore, the interaction between PIF4 and SEU could also involve an interaction with BZR1. SEU is a homolog of LEUNIG (LEU) and affects histone methylation status at target genes, suggesting that it interacts with HME. Presumably, the “active chromatin” state of the *YUCCA8* locus can be maintained as long as HDA9 protein activity is maintained. Upon return to 22°C HDA9 protein is no longer stabilized, resulting in re-acetylation of H3K9K14 at the *YUCCA8* locus and efficient incorporation of repressive H2A.Z. This likely limits access for BZR1, PIF4, and MED25, while at the same time nuclear levels of BZR1 and expression of PIF4 also decrease. In addition, the expression of HDA9 in germinating seedlings is transient (van der Woude et al., 2019). Finally, it was

suggested that MED25 is a negative regulator of PHYB/D/E (Wollenberg et al., 2008). If indeed MED25 reduces PHYB level/stability, the absence of MED25 is expected to correspond with increased PHYB level/stability, which in turn would reduce PIF4 protein stability. This may be part of the explanation why the higher transcription level of *PIF4* in *pft1-2* does not correspond with increased expression of *YUCCA8* and will be subject for future investigations.

Finally, during the submission of this manuscript, a similar role for MED14 during thermomorphogenesis was shown (Bajracharya et al., 2022). Similar to what is shown here for MED25, MED14 protein also interacts with PIF4 protein and shows enhanced presence at PIF4 gene targets at elevated temperatures. Indeed, a role for MED25 in hypocotyl elongation during thermomorphogenesis was demonstrated, but without going into details of this function of MED25 (Bajracharya et al., 2022). Therefore, thus far an impressive number of proteins have been identified that interact directly with PIF4 protein during thermomorphogenesis: PHYB (Yamashino et al., 2013), TOC1 (Zhu et al., 2016), HEMERA (Qiu et al., 2019), MED14 (Bajracharya et al., 2022), and MED25 (this paper). Disruption of the Mediator complex by the absence of key components like MED14 or MED25 could exert similar effects, but some Mediator mutants do not show specific effects during thermomorphogenesis (Bajracharya et al., 2022). MED25 binding to different types of transcription factors has been tested in high throughput screening (Ou et al., 2011) and MED25 shows selectivity for a specific subset of transcription factors (Table 1). While there clearly is an overlap in transcription factor targets between MED25 and MED14, a comprehensive screen for MED14 binding to different types of transcription factors has not been performed. More research is needed to unravel the interaction mechanism between all these proteins and the specificity imposed by different Mediator components during different growth responses in plants.

Materials and methods

Plant material and growth conditions

Arabidopsis (*Arabidopsis thaliana*) Col-0 wild-type genetic background was used for all experiments. All genotypes used are listed in Supplemental Table 1B. T-DNA insertion mutants were obtained from the Nottingham Arabidopsis Stock Centre (www.arabidopsis.info), and homozygous mutant genotypes were confirmed by PCR using gene-specific and T-DNA-specific primers (Supplemental Table 2). The double/triple mutant combinations were obtained by crossing and confirmed by PCR.

Seeds were first incubated for 3–4 days at 4°C in darkness. After cold treatment, the water-imbibed seeds were sown onto rock wool. Plants were then grown in cycles of 12 h light, 22°C/12 h darkness, and 12°C (unless specified

otherwise) on rock wool on half-strength Hoagland-nutrient solution. Growth experiments were under mixed (R, B, FR) LED lights with FR ramping at start and end of the photoperiod to mimic natural changes in FR light conditions at the start and end of the day (van Hoogdalem et al., 2021).

Plasmid constructs

For expression constructs, the full-length *PIF4*, *BZR1*, *HDA9*, and *MED25* CDS was amplified from a Col-0 cDNA library using gene-specific primers, including 5' overhang *Xba*I and 3' overhang *Not*I restriction sites (Supplemental Table 4). The expected PCR products were digested and ligated with T4 DNA ligase (#M1801, Promega, Madison, USA) into *pIV1A2.1* entry vector (Plant Research International, Wageningen, Netherlands) between the *CaMV35S* promoter and *RbcS1* terminator. For *MED25* with *cmv-His-tag*, the full-length *MED25* CDS was amplified using a specific primer set (without stop codon) including 5' overhang *Xba*I and 3' overhang *Not*I restriction sites. Then, the PCR product was digested and ligated into *pIV1A2.1-cmyc-His tag* entry vector. For the luciferase (*LUC*) reporter constructs, the promoter sequence for *YUCCA8* was used as predicted by (Sun et al., 2012). The fragment was amplified from gDNA using primers with 5' overhang *Asc*I and 3' overhang *Xba*I restriction sites (Table-S4). The PCR products were first digested with restriction enzymes and then ligated into *pIV1A2.1* entry vector in front of *LUC*. All entry vectors were then cloned into the Gateway-compatible binary vectors *pKGW-Red Seed* (<https://gatewayvectors.vib.be/>) or *pBA* by an LR reaction. Thereafter, the expression and reporter vectors (Supplemental Table 2) were transformed into the *Agrobacterium tumefaciens* AGL-0 strain, which was used in transient expression assays in *Nicotiana benthamiana* or was used for stable Arabidopsis (Col-0) transformation using the floral dip method as described before (Zhang et al., 2006). Transgenic Arabidopsis T0 seeds were identified by DsRed pigmentation of the seed coat or by *LUC*-reporter activity. Seeds were harvested from T1 plants and homozygous plants were selected based on Mendelian segregation of DsRed fluorescence in the progeny population(s). For each transformation, a representative homozygous line was selected from at least 10 primary transformants for further experiments.

For the split-*LUC* assays, *pDEST-cLuc* and *pDEST-nLuc* vectors were used as a backbone for the different fusion protein constructs (Chen et al., 2008) (see Supplemental Table 3). The entry vectors containing either full length of *HDA9* CDS, *PIF4* CDS, *BZR1* CDS, *MED25* CDS, or *MED25* domain sequences were cloned into *pDEST-cLuc* and *pDEST-nLuc* vectors respectively. As a negative control, the *35S:cLuc* (*pCAMBIA-cLuc*) and *35S:nLuc* (*pCAMBIA-nLuc*) expression constructs were used (Chen et al., 2008).

Hypocotyl elongation assays

Col-0, *pft1-2* (SALK_129555C), *pft1-3* (SALK_059316C), *hda9-1* (SALK_007123), *pft1-2/hda9-1* double mutant and

35S::MED25 OE seeds were gas sterilized and stratified at 4°C for 3 days. The seeds were then sown onto half-strength MS medium and placed into a climate chamber with mixed LEDs (blue B), red (R), and far-red (FR), under the following conditions: 20°C and 8 h light/16 h darkness. The photoperiod started with a ramping period in the first and last hour, with 30 $\mu\text{mol m}^{-2} \text{s}^{-1}$ and a B:R:FR ratio of 1:2:1. The remaining 6 h had 100 $\mu\text{mol m}^{-2} \text{s}^{-1}$ and B:R:FR ratio of 3:6:1 (van Hoogdalem et al., 2021). After 24 h of acclimatization, half of the plates were placed at 28°C (high-temperature treatment) for 8 days. After 8 days pictures of the plates were taken, and the hypocotyl was measured using ImageJ (Bethesda, Maryland, USA). A 2-way ANOVA followed by a TUKEY HSD post hoc test was used to statically compare the hypocotyl lengths.

Gene expression analysis by reverse transcription quantitative PCR (RT-qPCR)

Total RNA was isolated using homogenized young leaf tissues with the InviTrap® Spin Plant RNA Kit and treated with Ambion® TURBO DNA-free Kit according to the manufacturer's instructions. cDNA synthesis was performed using the iScript II mix reagent that included 10 mM oligo (dT) primer according to the manufacturer's instruction (Bio-Rad, CA, USA). RT-qPCR was performed using iQ SYBR Green Super mix (Bio-Rad, CA, USA) on a CFX Connect Real-Time System (Bio-Rad, CA, USA). The IPP2 was used as a reference for the normalization of relative expression levels. Gene expression levels were calculated from the average level detected in three biological replicate samples (pooled material from three plants per sample) (van Hoogdalem et al., 2021).

ChIP-qPCR assays

ChIP assays were performed as previously described (Bowler et al., 2004; Perrella et al., 2018; van der Woude et al., 2019). DNA was sheared using an ultrasonic bath (FALC instruments LABSONIC LBS2.10), cooled at 4°C using the maximum kHz frequency of 20 cycles 45 s ON, 15 s OFF. Anti-6XHis tag (Abcam ab9108) was used to IP the chromatin according to the manufacturer's instructions. ChIP-qPCR was performed using the following cycles: 95°C × 2 min, 95°C × 3 s, 59.5°C × 30 s for 50 cycles, 95°C × 1 min, and 60°C × 30 s to estimate the melting curve. Oligonucleotides for YUCCA8 and PIF4 DNA genomic regions were designed based on Lee et al. (2014) and Zhu et al. (2016). Relative ChIP DNA abundance was calculated as previously described (Kaiserli et al., 2015). In detail, MED25 enrichment over loci was determined by normalizing immuno-precipitated DNA against genomic DNA for the indicated regions and temperature conditions and indicated as a percentage of nuclear DNA (%Input). DNA was also immunoprecipitated from Col-0 wild-type plants and used as a negative control for ChIP-qPCR amplifications.

Imaging and quantification of *in planta* luciferase activity in Arabidopsis

For the imaging of LUC-reporter activity in stably transformed Arabidopsis plants, the plants were sprayed with 1 mM D-luciferin (Duchefa Biochemie, Haarlem, The Netherlands) 24 h prior to imaging to inactivate accumulated luciferase protein. Spraying with D-luciferin was repeated 1 h before imaging. Imaging was performed with our LUMINATOR setup consisting of an air-cooled (−80°C) CCD Pixis 1024B camera system (Princeton Instruments, Massachusetts, USA) equipped with a 35 mm, 1:1.4 Nikon SLR camera lens (Nikon, Tokyo, Japan) fitted with a DT Green filter ring (Image Optics Components Ltd, Orsay, France) to block chlorophyll fluorescence (van Hoogdalem et al., 2021). Exposure time for the LUC activity measurements is as indicated in the figure legend. In the diurnal LUC activity experiment, spraying with D-luciferin was repeated once a day. For each reporter line, the average LUC activity is indicated from at least eight individual plants. Relative luminescence from LUC activity was quantified from images using ImageJ (Bethesda, Maryland, USA), using background subtraction (van Hoogdalem et al., 2021). Note that the resulting numbers do not represent the number of photons produced by LUC activity, but rather a “gray” value in arbitrary units and the graphs present the changes in these arbitrary units relative to those of the first image in the image sequence. Quantification of the *in planta* LUC activity depends on tissue size, distance to camera, and exposure time. Within each experiment, these were held constant, but between experiments they may differ. The quantification of LUC activity (as determined from the “gray value” in the image) is given as relative units: Relative LUC activity. For Figures 2C and 7, A and B the average LUC activity in four groups of at least ten seedlings was quantified. For Figure 2F ($n = 6$), Figure 4F ($n = 5$), Figure 6G ($n = 6$) the average LUC activity in n independently infiltrated leaf discs of *N. benthamiana*, was quantified at 3 days post-agroinfiltration. For Figure 3B YUCCA8::LUC activity was quantified in extracts of at least eight independently infiltrated leaf discs of *N. benthamiana* leaves and normalized to the Renilla LUC activity from the co-infiltrated 35S::Renilla LUC construct (ffLUC/rLUC).

Transient expression assays using agro-infiltration in *N. benthamiana* leaves

To probe YUCCA8 transcriptional activity, *N. benthamiana* leaves were agro-infiltrated with the pYUCCA8::LUC-reporter and -effector construct 35S::PIF4, with or without the 35S::MED25 expression construct. Relative gene dosage of the different expression constructs was kept equal by complementing the agro-infiltration with an Agrobacterium containing an EV construct when necessary. Agro-infiltration also included a P19 expression construct to suppress gene silencing (Saxena et al., 2011) and a 35S::Renilla luciferase expression construct for normalization of agro-infiltration

efficiency. At least six leaves were agro-infiltrated per treatment. After 4 days, the co-infiltrated leaves were harvested for further analysis. From each leaf, three disks (1 cm size) of infiltrated material were taken as technical replicates. Leaf disks were frozen and grinded in liquid nitrogen and 200 μl of passive lysis buffer was added to each sample, vortexed and after 10–15 min on ice, samples were vortexed again and leaf residue was pelleted. For each sample, 100 μl supernatant was pipetted into the 96-wells plate for measurement of Firefly- and *Renilla* luciferase activity according to the specifications of the Promega dual luciferase assay kit in a Glomax microplate reader. Relative Firefly luciferase activity in different samples was normalized to the *Renilla* LUC activity in each sample.

Yeast-two-hybrid assay

Full-length *HDA9* and *MED25* were cloned into Gateway-compatible *pDonr/Zeo* vector via a BP reaction. The *pDONR-HDA9* was then cloned into the *pGAD424-GW* vector and the *pDONR-MED25* was cloned into *pGBT9-GW* vector using LR clonase, to generate *AD-HDA9* and *BD-MED25*. Both constructs were transformed into the yeast *AH109* strain by the lithium acetate method according to the manufacturer's instructions (Clontech). Positive yeast colonies were plated on SD medium lacking Leu and Trp (–2aa) and SD medium lacking His, Ade, Leu, and Trp (–4aa) to test for protein interactions. The plates were incubated at 30°C for 3 days.

Bimolecular fluorescence complementation assays

Full-length *HDA9* and *MED25* were cloned into *pBA3134* and *pBA3132* by Gateway cloning to generate *nYFP-HDA9* and *MED25-cYFP* vectors, respectively (Seo et al., 2017). *nYFP-6xmyc* and *6xmyc-cYFP* vectors were used as a negative control. Destination constructs were transformed into *Agrobacterium tumefaciens* strain GV3101. Cultured *nYFP-HDA9* and *MED25-cYFP* *Agrobacterium* cells were co-infiltrated with P19 and mCherry^{NLS} *Agrobacterium* cells into leaves of 3-week-old *Nicotiana benthamiana* plants. YFP fluorescence signals were detected using an Olympus FV3000RS confocal laser scanning microscope (Olympus) 3 days after infiltration. Two types of filters were used: mCHERRY, excitation 587 nm, emission 610 nm; EYFP, excitation 490–510 nm, emission 520–550 nm. Exposure time was 5.22 ms for all experiments. The images were captured with a 20 \times and 40 \times objective lenses.

Split-luciferase assays in *N. benthamiana* leaves

Split luciferase assays were performed by transient expression in *N. benthamiana*. Expression constructs were transformed to *Agrobacterium tumefaciens* strain AGL-0 and grown at 27°C in an LB medium containing 10 $\mu\text{g ml}^{-1}$ Rifampicin and 50 $\mu\text{g ml}^{-1}$ kanamycin. The *Agrobacterium tumefaciens* cells were resuspended in agro-infiltration buffer including 10 mM MES (2-morpholino ethanesulfonic acid, Duchefa Biochemie, Haarlem, NL), 10 mM MgCl₂, and 100 mM

acetosyringone (4'-hydroxy-3',5'-dimethoxyacetophenone, Sigma Aldrich, USA) and incubated at room temperature for 3 h under modest shaking. For the assay an equal volume of two *Agrobacterium* strains (OD₆₀₀ = 0.3) was mixed and co-infiltrated into 5-week-old *N. benthamiana* leaves. At least 6 *N. benthamiana* leaves were used for each tested combination. After 72 h post-agroinfiltration the leaves were harvested. For the imaging of LUC activity, the leaves were sprayed with 1 mM D-luciferin at 24 and 1 h before imaging. LUC activity was captured using the previously described LUMINATOR setup using 7 min of exposure. The relative LUC activity in the images was quantified by ImageJ software (Bethesda, Maryland, USA).

Immunoblotting

Seedlings expressing 35S:eGFP-HDA9 were grown at 22°C. After 7 days seedlings were transferred to a medium containing MG132 (50 μM) or DMSO (control) for another 4 h at 22°C light or dark and 27°C light or dark, respectively. Total proteins were extracted in buffer containing 100 mM Tris-HCl [pH 7.5], 300 mM NaCl, 2 mM EDTA [pH 8.0], 1% Triton X-100 v/v, 10% glycerol v/v, 50 μM MG132, and protease inhibitor. Proteins were size-separated on 10% SDS-PAGE gel. eGFP-HDA9 fusion protein (75 kDa) was detected on a western blot using antibodies against GFP protein (50430-2-AP, Proteintech, 1:5000). The signal of the eGFP protein on the western blot was normalized to that of the Rubisco staining on the blot. Signals were quantified in Image J.

Co-immunoprecipitation assay in *A. thaliana*

Homozygous 35S:*MED25-myc*, 35S:*PIF4-HA*, and the heterozygous F1 generation of 35S:*MED25-myc* 35S:*PIF4-HA* transgenic lines were used for Co-IP experiments. Ten-day-old transgenic seedlings were grown under white light at 22°C and transferred to 27°C for overnight exposure, before extraction of protein. About 40 seedlings were ground in liquid nitrogen and resuspended in 500 μl IP buffer (50 mM Tris-HCl pH 7.5, 1 mM ethylenediaminetetraacetic acid [EDTA], 75 mM NaCl, 0.5% v/v Triton X-100, 5% Glycerol v/v, 2 mM DTT, and 1 mM protease inhibitor mixture). After centrifugation at 14,000g for 10 min under 4 °C, the supernatant was mixed with 50 μl Anti-HA Magnetic Beads (Cat#: 88836, Thermo Fisher Scientific) and incubated at 4 °C for 2 h. The beads were washed five times with washing buffer (50 mM Tris-HCl pH 8.0, 150 mM NaCl, and 0.1% Triton X-100 v/v) and eluted with a 2 \times SDS loading buffer at 95 °C for 10 min. Immunoprecipitated products were detected using western blotting with anti-MYC (cat#16286-1-AP, Proteintech, 1:3000), or anti-HA (sc-7392, Santa Cruz Biotechnology, 1:500) monoclonal antibodies.

Accession numbers

Accession number of all genes mentioned in this paper can be found in [Supplemental Table 1A](#).

Supplemental data

The following materials are available in the online version of this article.

Supplemental Figure S1. MED25 affects the growth of *Arabidopsis*.

Supplemental Figure S2. Mapping of various proteins along the MED25 protein sequence known to physically interact with different MED25 domains.

Supplemental Figure S3. Interaction MED25, PIF4, and HDA9 not additive in split-LUC assay

Supplemental Figure S4. 35S-HDA9-LUC-reporter expression in WT, pft1-2, and MED25OE and 35S-LUC activity at 22°C and 27°C.

Supplemental Figure S5. Repeat of the experiment shown in Figure 7C.

Supplemental Figure S6. Split-LUC assays for the interaction between MED25 and BZR1.

Supplemental Table S1. List of mutant and reporter lines studied in this work.

Supplemental Table S2. Putative PIF4 binding sites at the *PIF4* and *YUCCA8* promoter according to Plant Pan 3.0 (Chow et al., 2019).

Supplemental Table S3. List of expression constructs used in transient expression assays.

Supplemental Table S4. List of primers used in this work.

Funding

U.S. was supported by Erasmus Mundus Action 2 project TIMUR (Training of Individuals through Mobility from Uzbek Republic to European Union). A.R.v.d.K. acknowledges the research program Compact Plants (13149), which is (partly) financed by the Netherlands Organisation for Scientific Research.

Acknowledgments

We thank Marielle Schreuder for her technical support and excellent care of plants.

Conflict of interest statement. None declared.

References

- Am C, Li L, Zhai Q, You Y, Deng L, Wu F, Chen R, Jiang H, Wang H, Chen Q, et al. (2017) Mediator subunit MED25 links the jasmonate receptor to transcriptionally active chromatin. *Proc Natl Acad Sci U S A* **114**(42): E8930–E8939
- Backstrom S, Elfving N, Nilsson R, Wingsle G, Bjorklund S (2007) Purification of a plant mediator from *Arabidopsis thaliana* identifies PFT1 as the Med25 subunit. *Mol Cell* **26**(5): 717–729
- Bai M-Y, Shang J-X, Oh E, Fan M, Bai Y, Zentella R, Sun T-P, Wang Z-Y (2012) Brassinosteroid, gibberellin and phytochrome impinge on a common transcription module in *Arabidopsis*. *Nat Cell Biol* **14**(8): 810–817
- Bajracharya A, Xi J, Grace KF, Bayer EE, Grant CA, Clutton CH, Baerson SR, Agarwal AK, Qiu Y (2022) PHYTOCHROME-INTERACTING

- FACTOR 4/HEMERA-mediated thermosensory growth requires the mediator subunit MED14. *Plant Physiol* **190**(4): 2706–2721
- Bellaet J, Trenner J, Lippmann R, Poeschl Y, Zhang X, Friml J, Quint M, Delker C (2019) A mobile auxin signal connects temperature sensing in cotyledons with growth responses in hypocotyls. *Plant Physiol* **180**(2): 757–766
- Bours R, Kohlen W, Bouwmeester HJ, Van Der Krol A (2015) Thermoperiodic control of hypocotyl elongation depends on auxin-induced ethylene signaling that controls downstream PHYTOCHROME INTERACTING FACTOR3 activity. *Plant Physiol* **167**(2): 517–530
- Bours R, Van Zanten M, Pierik R, Bouwmeester H, Van Der Krol A (2013) Antiphase light and temperature cycles affect PHYTOCHROME B-controlled ethylene sensitivity and biosynthesis, limiting leaf movement and growth of *Arabidopsis*. *Plant Physiol* **163**(2): 882–895
- Bowler C, Benvenuto G, Laflamme P, Molino D, Probst AV, Tariq M, Paszkowski J (2004) Chromatin techniques for plant cells. *Plant J* **39**(5): 776–789
- Box MS, Huang BE, Domijan M, Jaeger KE, Khattak AK, Yoo SJ, Sedivy EL, Jones DM, Hearn TJ, Webb AAR, et al. (2015) ELF3 Controls thermoresponsive growth in *Arabidopsis*. *Curr Biol* **25**(2): 194–199
- Burko Y, Willige BC, Seluzicki A, Novák O, Ljung K, Chory J (2022) PIF7 is a master regulator of thermomorphogenesis in shade. *Nat Commun* **13**(1): 4942
- Casal JJ, Balasubramanian S (2019) Thermomorphogenesis. *Annu Rev Plant Biol* **70**(1): 321–346
- Castroverde CDM, Dina D (2021) Temperature regulation of plant hormone signaling during stress and development. *J Exp Bot* <https://doi.org/10.1093/jxb/erab257>
- Cerdan PD, Chory J (2003) Regulation of flowering time by light quality. *Nature* **423**(6942): 881–885
- Cevik V, Kidd BN, Zhang P, Hill C, Kiddle S, Denby KJ, Holub EB, Cahill DM, Manners JM, Schenk PM, et al. (2012) MEDIATOR25 acts as an integrative hub for the regulation of jasmonate-responsive gene expression in *Arabidopsis*. *Plant Physiol* **160**(1): 541–555
- Chen H, Zou Y, Shang Y, Lin H, Wang Y, Cai R, Tang X, Zhou J-M (2008) Firefly luciferase complementation imaging assay for protein-protein interactions in plants. *Plant Physiol* **146**(2): 368
- Chen R, Jiang H, Li L, Zhai Q, Qi L, Zhou W, Liu X, Li H, Zheng W, Sun J, et al. (2012) The *Arabidopsis* mediator subunit MED25 differentially regulates jasmonate and abscisic acid signaling through interacting with the MYC2 and ABI5 transcription factors. *Plant Cell* **24**(7): 2898–2916
- Chen X, Lu L, Mayer KS, Scalf M, Qian S, Lomax A, Smith LM, Zhong X (2016) POWERDRESS interacts with HISTONE DEACETYLASE 9 to promote aging in *Arabidopsis*. *Elife* **5**: e17214
- Chow C-N, Lee T-Y, Hung Y-C, Li G-Z, Tseng K-C, Liu Y-H, Kuo P-L, Zheng H-Q, Chang W-C (2019) PlantPAN3.0: a new and updated resource for reconstructing transcriptional regulatory networks from ChIP-seq experiments in plants. *Nucleic Acids Res* **47**(D1): D1155–D1163
- Crawford AJ, Mclachlan DH, Hetherington AM, Franklin KA (2012) High temperature exposure increases plant cooling capacity. *Curr Biol* **22**(10): R396–R397
- De Rooij PGH, Perrella G, Kaiserli E, Van Zanten M (2020) The diverse and unanticipated roles of histone deacetylase 9 in coordinating plant development and environmental acclimation. *J Exp Bot* **71**(20): 6211–6225
- Delker C, Sonntag L, James GV, Janitza P, Ibanez C, Ziermann H, Peterson T, Denk K, Mull S, Ziegler J, et al. (2014) The DET1-COP1-HY5 pathway constitutes a multipurpose signaling module regulating plant photomorphogenesis and thermomorphogenesis. *Cell Rep* **9**(6): 1983–1989
- Elfving N, Davoine C, Benlloch R, Blomberg J, Brannstrom K, Muller D, Nilsson A, Ulfstedt M, Ronne H, Wingsle G, et al. (2011) The

- Arabidopsis thaliana* Med25 mediator subunit integrates environmental cues to control plant development. *Proc Natl Acad Sci U S A* **108**(20): 8245–8250
- Flanagan PM, Kelleher RJ 3rd, Sayre MH, Tschochner H, Kornberg RD** (1991). A mediator required for activation of RNA polymerase II transcription in vitro. *Nature* **350**(6317): 436–438
- Franklin KA, Lee SH, Patel D, Kumar SV, Spartz AK, Gu C, Ye S, Yu P, Breen G, Cohen JD, et al.** (2011) Phytochrome-interacting factor 4 (PIF4) regulates auxin biosynthesis at high temperature. *Proc Natl Acad Sci U S A* **108**(50): 20231–20235
- Gangappa SN, Berriri S, Kumar SV** (2017) PIF4 Coordinates thermosensory growth and immunity in *Arabidopsis*. *Curr Biol* **27**(2): 243–249
- Gray WM, Ostin A, Sandberg G, Romano CP, Estelle M** (1998) High temperature promotes auxin-mediated hypocotyl elongation in tomato. *Plant Physiol* **184**(3): 1217–1218
- Hartman S** (2020) MED25 mediates shade-induced hypocotyl elongation in tomato. *Plant Physiol* **184**(3): 1217–1218
- Huai J, Zhang X, Li J, Ma T, Zha P, Jing Y, Lin R** (2018) SEUSS and PIF4 coordinately regulate light and temperature signaling pathways to control plant growth. *Mol Plant* **11**(7): 928–942
- Huq E, Quail PH** (2002) PIF4, a phytochrome-interacting bHLH factor, functions as a negative regulator of phytochrome B signaling in *Arabidopsis*. *EMBO J* **21**(10): 2441–2450
- Hussein NK, Sabr LJ, Lobo E, Booth J, Ariens E, Detchanamurthy S, Schenk PM** (2020) Suppression of *Arabidopsis* mediator subunit-encoding *MED18* confers broad resistance against DNA and RNA viruses while *MED25* is required for virus defense. *Front Plant Sci* **11**: 162
- Ibanez C, Delker C, Martinez C, Burstenbinder K, Janitza P, Lippmann R, Ludwig W, Sun H, James GV, Klecker M, et al.** (2018) Brassinosteroids dominate hormonal regulation of plant thermomorphogenesis via BZR1. *Curr Biol* **28**(2): 303–310.e3
- Inigo S, Alvarez MJ, Strasser B, Califano A, Cerdan PD** (2012) PFT1, The MED25 subunit of the plant mediator complex, promotes flowering through CONSTANS dependent and independent mechanisms in *Arabidopsis*. *Plant J* **69**(4): 601–612
- Inigo S, Giraldez AN, Chory J, Cerdan PD** (2012) Proteasome-mediated turnover of *Arabidopsis* MED25 is coupled to the activation of FLOWERING LOCUS T transcription. *Plant Physiol* **160**(3): 1662–1673
- Ito J, Fukaki H, Onoda M, Li L, Li C, Tasaka M, Furutani M** (2016) Auxin-dependent compositional change in mediator in ARF7- and ARF19-mediated transcription. *Proc Natl Acad Sci U S A* **113**(23): 6562–6567
- Kaiserli E, Paldi K, O'Donnell L, Batalov O, Pedmale UV, Nusinow DA, Kay SA, Chory J** (2015) Integration of light and photoperiodic signaling in transcriptional nuclear foci. *Dev Cell* **35**(3): 311–321
- Kazan K** (2017) The multitasking MEDIATOR25. *Front Plant Sci* **8**: 999
- Kidd BN, Aitken EA, Schenk PM, Manners JM, Kazan K** (2010) Plant mediator: mediating the jasmonate response. *Plant Signal Behav* **5**(6): 718–720
- Kidd BN, Cahill DM, Manners JM, Schenk PM, Kazan K** (2011) Diverse roles of the mediator complex in plants. *Semin Cell Dev Biol* **22**(7): 741–748
- Kidd BN, Edgar CI, Kumar KK, Aitken EA, Schenk PM, Manners JM, Kazan K** (2009) The mediator complex subunit PFT1 is a key regulator of jasmonate-dependent defense in *Arabidopsis*. *Plant Cell* **21**(8): 2237–2252
- Kim S, Hwang G, Kim S, Thi TN, Kim H, Jeong J, Kim J, Kim J, Choi G, Oh E** (2020) The epidermis coordinates thermoresponsive growth through the phyB-PIF4-auxin pathway. *Nat Commun* **11**(1): 1053
- Kim Y-J, Bjorklund S, Li Y, Sayre MH, Kornberg RD** (1994) A multi-protein mediator of transcriptional activation and its interaction with the C-terminal repeat domain of RNA polymerase II. *Cell* **77**(4): 599–608
- Klose C, Buche C, Fernandez AP, Schafer E, Zwick E, Kretsch T** (2012) The mediator complex subunit PFT1 interferes with COP1 and HY5 in the regulation of *Arabidopsis* light signaling. *Plant Physiol* **160**(1): 289–307
- Koini MA, Alvey L, Allen T, Tilley CA, Harberd NP, Whitelam GC, Franklin KA** (2009) High temperature-mediated adaptations in plant architecture require the bHLH transcription factor PIF4. *Curr Biol* **19**(5): 408–413
- Kumar SV, Lucyshyn D, Jaeger KE, Alos E, Alvey E, Harberd NP, Wigge PA** (2012) Transcription factor PIF4 controls the thermosensory activation of flowering. *Nature* **484**(7393): 242–245
- Lee HJ, Jung JH, Cortés Llorca L, Kim S-J, Lee S, Baldwin IT, Park C-M** (2014) FCA mediates thermal adaptation of stem growth by attenuating auxin action in *Arabidopsis*. *Nat Commun* **5**: 5473. <https://doi.org/10.1038/ncomms6473>
- Liu J, Cheng X, Liu P, Li D, Chen T, Gu X, Sun J** (2017) MicroRNA319-regulated TCPs interact with FBHs and PFT1 to activate CO transcription and control flowering time in *Arabidopsis*. *PLoS Genet* **13**(5): e1006833
- Lorrain S, Allen T, Duek PD, Whitelam GC, Fankhauser C** (2008) Phytochrome-mediated inhibition of shade avoidance involves degradation of growth-promoting bHLH transcription factors. *Plant J* **53**(2): 312–323
- Ma L, Li G** (2019) Auxin-dependent cell elongation during the shade avoidance response. *Front Plant Sci* **10**: 914
- Matzke AJ, Matzke MA** (1998) Position effects and epigenetic silencing of plant transgenes. *Curr Opin Plant Biol* **1**(2): 142–148
- Mayer KS, Chen X, Sanders D, Chen J, Jiang J, Nguyen P, Scalf M, Smith LM, Zhong X** (2019) HDA9-PWR-HOS15 is a core histone deacetylase Complex regulating transcription and development. *Plant Physiol* **180**(1): 342–355
- Muller-Moule P, Nozue K, Pytlak ML, Palmer CM, Covington MF, Wallace AD, Harmer SL, Maloof JN** (2016) YUCCA Auxin biosynthetic genes are required for *Arabidopsis* shade avoidance. *PeerJ* **4**: e2574
- Nusinow DA, Helfer A, Hamilton EE, King JJ, Imaizumi T, Schultz TF, Farre EM, Kay SA** (2011) The ELF4-ELF3-LUX complex links the circadian clock to diurnal control of hypocotyl growth. *Nature* **475**(7356): 398–402
- Oh E, Zhu J-Y, Wang Z-Y** (2012) Interaction between BZR1 and PIF4 integrates brassinosteroid and environmental responses. *Nat Cell Biol* **14**(8): 802–809
- Ou B, Yin K-Q, Liu S-N, Yang Y, Gu T, Wing Hui JM, Zhang L, Miao J, Kondou Y, Matsui M, et al.** (2011) A high-throughput screening system for *Arabidopsis* transcription factors and its application to Med25-dependent transcriptional regulation. *Mol Plant* **4**(3): 546–555
- Perrella G, Baurle I, Van Zanten M** (2022) Epigenetic regulation of thermomorphogenesis and heat stress tolerance. *New Phytol* **234**(4): 1144–1160
- Perrella G, Davidson MLH, O'Donnell L, Nastase AM, Herzyk P, Breton G, Pruneda-Paz JL, Kay SA, Chory J, Kaiserli E** (2018) ZINC-FINGER interactions mediate transcriptional regulation of hypocotyl growth in *Arabidopsis*. *Proc Natl Acad Sci U S A* **115**(19): E4503–E4511
- Perrella G, Lopez-Vernaza MA, Carr C, Sani E, Gossele V, Verduyn C, Kellermeier F, Hannah MA, Amtmann A** (2013) Histone deacetylase complex1 expression level titrates plant growth and abscisic acid sensitivity in *Arabidopsis*. *Plant Cell* **25**(9): 3491–3505
- Qiu Y, Li M, Kim RJ, Moore CM, Chen M** (2019) Daytime temperature is sensed by phytochrome B in *Arabidopsis* through a transcriptional activator HEMERA. *Nat Commun* **10**(1): 140
- Quint M, Delker C, Franklin KA, Wigge PA, Halliday KJ, Van Zanten M** (2016) Molecular and genetic control of plant thermomorphogenesis. *Nat Plants* **2**(1): 15190
- Raschke A, Ibanez C, Ullrich KK, Anwer MU, Becker S, Glockner A, Trenner J, Denk K, Saal B, Sun X, et al.** (2015) Natural variants of ELF3 affect thermomorphogenesis by transcriptionally modulating PIF4-dependent auxin response genes. *BMC Plant Biol* **15**(1): 197

- Rival P, Press MO, Bale J, Grancharova T, Undurraga SF, Queitsch C (2014) The conserved PFT1 tandem repeat is crucial for proper flowering in *Arabidopsis thaliana*. *Genetics* **198**(2): 747–754
- Samanta S, Thakur JK (2015) Importance of mediator complex in the regulation and integration of diverse signaling pathways in plants. *Front Plant Sci* **6**: 757
- Saxena P, Hsieh Y-C, Alvarado VY, Sainsbury F, Saunders K, Lomonosoff GP, Scholthof HB (2011) Improved foreign gene expression in plants using a virus-encoded suppressor of RNA silencing modified to be developmentally harmless. *Plant Biotechnol J* **9**(6): 703–712
- Seguela-Arnaud M, Smith C, Uribe MC, May S, Fischl H, Mckenzie N, Bevan MW (2015) The mediator complex subunits MED25/PFT1 and MED8 are required for transcriptional responses to changes in cell wall arabinose composition and glucose treatment in *Arabidopsis thaliana*. *BMC Plant Biol* **15**(1): 215
- Seo JS, Sun H-X, Park BS, Huang C-H, Yeh S-D, Jung C, Chua N-H (2017) ELF18-INDUCED LONG-NONCODING RNA associates with mediator to enhance expression of innate immune response genes in *Arabidopsis*. *Plant Cell* **29**(5): 1024–1038
- Soutourina J (2018) Transcription regulation by the mediator complex. *Nat Rev Mol Cell Biol* **19**(4): 262–274
- Sun J, Qi L, Li Y, Chu J, Li C (2012) PIF4-mediated activation of YUCCA8 expression integrates temperature into the auxin pathway in regulating *Arabidopsis* hypocotyl growth. *PLoS Genet* **8**(3): e1002594
- Sun W, Han H, Deng L, Sun C, Xu Y, Lin L, Ren P, Zhao J, Zhai Q, Li C (2020) Mediator subunit MED25 physically interacts with PHYTOCHROME INTERACTING FACTOR4 to regulate shade-induced hypocotyl elongation in tomato. *Plant Physiol* **184**(3): 1549–1562
- Tasset C, Singh Yadav A, Sureshkumar S, Singh R, Van Der Woude L, Nekrasov M, Tremethick D, Van Zanten M, Balasubramanian S (2018) POWERDRESS-mediated histone deacetylation is essential for thermomorphogenesis in *Arabidopsis thaliana*. *PLoS Genet* **14**(3): e1007280
- Tian L, Fong MP, Wang JJ, Wei NE, Jiang H, Doerge RW, Chen ZJ (2005) Reversible histone acetylation and deacetylation mediate genome-wide, promoter-dependent and locus-specific changes in gene expression during plant development. *Genetics* **169**(1): 337–345
- Van Der Woude LC, Perrella G, Snoek BL, Van Hoogdalem M, Novak O, Van Verk MC, Van Kooten HN, Zorn LE, Tonckens R, Dongus JA, et al. (2019) HISTONE DEACETYLASE 9 stimulates auxin-dependent thermomorphogenesis in *Arabidopsis thaliana* by mediating H2A.Z depletion. *Proc Natl Acad Sci U S A* **116**(50): 25343–25354
- Van Hoogdalem M, Shapulatov U, Sergeeva L, Busscher-Lange J, Schreuder M, Jamar D, Van Der Krol AR (2021) A temperature regime that disrupts clock-controlled starch mobilization induces transient carbohydrate starvation, resulting in compact growth. *J Exp Bot* <https://doi.org/10.1093/jxb/erab075>
- Wollenberg AC, Strasser B, Cerdan PD, Amasino RM (2008) Acceleration of flowering during shade avoidance in *Arabidopsis* alters the balance between FLOWERING LOCUS C-mediated repression and photoperiodic induction of flowering. *Plant Physiol* **148**(3): 1681–1694
- Xu R, Li Y (2011) Control of final organ size by mediator complex subunit 25 in *Arabidopsis thaliana*. *Development* **138**(20): 4545–4554
- Yamashino T, Nomoto Y, Lorrain S, Miyachi M, Ito S, Nakamichi N, Fankhauser C, Mizuno T (2013) Verification at the protein level of the PIF4-mediated external coincidence model for the temperature-adaptive photoperiodic control of plant growth in *Arabidopsis thaliana*. *Plant Signal Behav* **8**(3): e23390
- Yang Y, Ou B, Zhang J, Si W, Gu H, Qin G, Qu L-J (2014) The *Arabidopsis* mediator subunit MED16 regulates iron homeostasis by associating with EIN3/EIL1 through subunit MED25. *Plant J* **77**(6): 838–851
- Yao T, Park BS, Mao H-Z, Seo JS, Ohama N, Li Y, Yu N, Mustafa NFB, Huang C-H, Chua N-H (2019) Regulation of flowering time by SPL10/MED25 module in *Arabidopsis*. *New Phytol* **224**(1): 493–504
- You Y, Zhai Q, An C, Li C (2019) LEUNIG_HOMOLOG mediates MYC2-dependent transcriptional activation in cooperation with the coactivators HAC1 and MED25. *Plant Cell* **31**(9): 2187–2205
- Zhang F, Yao J, Ke J, Zhang L, Lam VQ, Xin X-F, Zhou XE, Chen J, Brunzelle J, Griffin PR, et al. (2015) Structural basis of JAZ repression of MYC transcription factors in jasmonate signalling. *Nature* **525**(7568): 269–273
- Zhang H, Zheng D, Yin L, Song F, Jiang M (2021) Functional analysis of OsMED16 and OsMED25 in response to biotic and abiotic stresses in rice. *Front Plant Sci* **12**: 652453
- Zhang X, Henriques R, Lin S-S, Niu Q-W, Chua N-H (2006) Agrobacterium-mediated transformation of *Arabidopsis thaliana* using the floral dip method. *Nat Protoc* **1**(2): 641–646
- Zhou Y, Xun Q, Zhang D, Lv M, Ou Y, Li J (2019) TCP transcription factors associate with PHYTOCHROME INTERACTING FACTOR 4 and CRYPTOCHROME 1 to regulate thermomorphogenesis in *Arabidopsis thaliana*. *iScience* **15**: 600–610
- Zhu J-Y, Oh E, Wang T, Wang Z-Y (2016) TOC1-PIF4 interaction mediates the circadian gating of thermoresponsive growth in *Arabidopsis*. *Nat Commun* **7**(1): 13692. <https://doi.org/10.1038/ncomms13692>
- Zhu Y, Schluttenhoffer CM, Wang P, Fu F, Thimmapuram J, Zhu JK, Lee SY, Yun DJ, Mengiste T (2014) CYCLIN-DEPENDENT KINASE8 differentially regulates plant immunity to fungal pathogens through kinase-dependent and -independent functions in *Arabidopsis*. *Plant Cell* **26**(10): 4149–4170